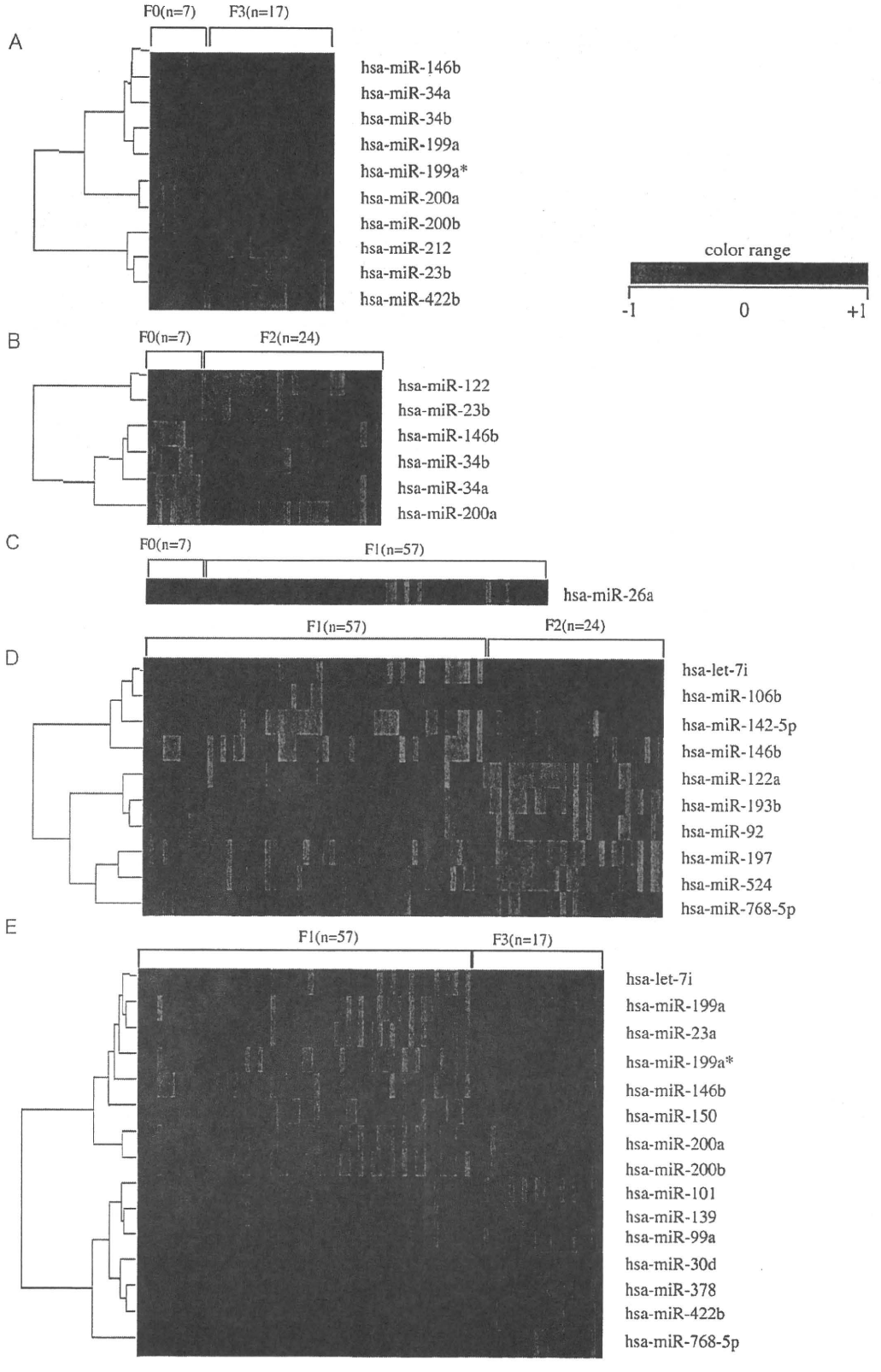
A
F0(n=7)
F3(n=17)
hsa-miR-146b
hsa-miR-34a
hsa-miR-34b
hsa-miR-199a
hsa-miR-199a*
hsa-miR-200a
hsa-miR-200b
hsa-miR-212
hsa-miR-23b
hsa-miR-422b
color range
-1
0
+1
B
F0(n=7)
F2(n=24)
hsa-miR-122
hsa-miR-23b
hsa-miR-146b
hsa-miR-34b
hsa-miR-34a
hsa-miR-200a
C
F0(n=7)
F1(n=57)
hsa-miR-26a
D
F1(n=57)
F2(n=24)
hsa-let-7i
hsa-miR-106b
hsa-miR-142-5p
hsa-miR-146b
hsa-miR-122a
hsa-miR-193b
hsa-miR-92
hsa-miR-197
hsa-miR-524
hsa-miR-768-5p
E
F1(n=57)
F3(n=17)
hsa-let-7i
hsa-miR-199a
hsa-miR-23a
hsa-miR-199a*
hsa-miR-146b
hsa-miR-150
hsa-miR-200a
hsa-miR-200b
hsa-miR-101
hsa-miR-139
hsa-miR-99a
hsa-miR-30d
hsa-miR-378
hsa-miR-422b
hsa-miR-768-5p

Figure 2. Liver fibrosis in human liver biopsy specimen. A. B. C. D. and E. miRNAs whose expression differs significantly between F0 and F3, F0 and F1, F0 and F2, F1 and F2, and F1 and F3, respectively. Relative expression level of each miRNA in human liver biopsy specimen by microarray. Data from microarray were also statistically analyzed using Welch's test and the Bonferroni correction for multiple hypotheses testing. Fold change, p-value are listed in Table S2.
doi:10.1371/journal.pone.0016081.g002

specific E3 ubiquitin protein ligase 2 (SMURF2), both of which play roles in the TGFβ signaling pathway, are candidate targets of miR-199a* and miR-200b, respectively, as determined by the Targetscan algorithm. The expression of miR-199a* was silenced in several proliferating cell lines excluding fibroblasts [21]. Down regulation of miR-199a, miR-199a* and 200a in chronic liver injury tissue was associated with the hepatocarcinogenesis [9]. miR-199a* is also one of the negative regulators of the HCV replication [22]. According to three target search algorithms (Pictar, miRanda, and Targetscan), the miRNAs that may be associated with the liver fibrosis can regulate several fibrosis-related genes (Table S4). Aberrant expression of these miRNAs may be closely related to the progress of the chronic liver disease.

Epithelial-mesenchymal transition (EMT) describes a reversible series of events during which an epithelial cell loses cell-cell contacts and acquires mesenchymal characteristics [23]. Although EMT is not a common event in adults, this process has been implicated in such instances as wound healing and fibrosis. Recent reports showed that the miR-200 family regulated EMT by targeting EMT accelerator ZEB1 and SIP1 [24]. From our observations, overexpression of miR-200a and miR-200b can be connected to the progression of liver fibrosis.

The diagnosis and quantification of fibrosis have traditionally relied on liver biopsy, and this is still true at present. However, there are a number of drawbacks to biopsy, including the invasive nature of the procedure and inter-observer variability. A number of staging systems have been developed to reduce both the inter-observer variability and intra-observer variability, including the METAVIR, the Knodell fibrosis score, and the Scheuer score. However, the reproducibility of hepatic fibrosis and inflammatory activity is not as consistent [25]. In fact, in our study, the degree of fibrosis of the two arbitrary fibrosis groups was classified using the miRNA expression profile with 80% or greater accuracy (data not shown). Thus, miRNA expression can be used for diagnosis of liver fibrosis.

In this study we investigated whether common miRNAs in human and mouse could influence the progression of the liver fibrosis. The signature of miRNAs expression can also serves as a tool for understanding and investigating the mechanism of the onset and progression of liver fibrosis. The miRNA expression profile has the potential to be a novel biomarker of liver fibrosis.

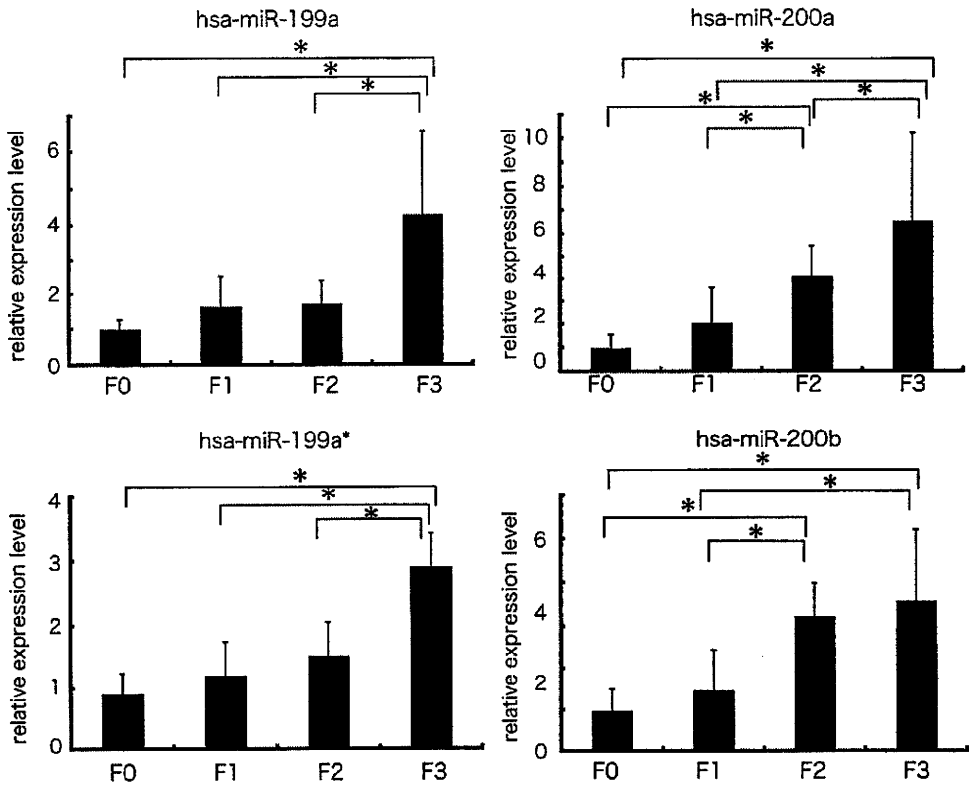

Figure 3. The expression level of miR-199 and 200 families in human liver biopsy specimen by real-time qPCR. Real-time qPCR validation of the 4 miRNAs (miR-199a, miR-199a*, miR-200a, and miR-200b). Each column represents the relative amount of miRNAs normalized to the expression level of U18. The data shown are the means+SD of three independent experiments. Asterisks indicates to a significant difference of $p<0.05$ (two-tailed Student-t test), respectively.
doi:10.1371/journal.pone.0016081.g003

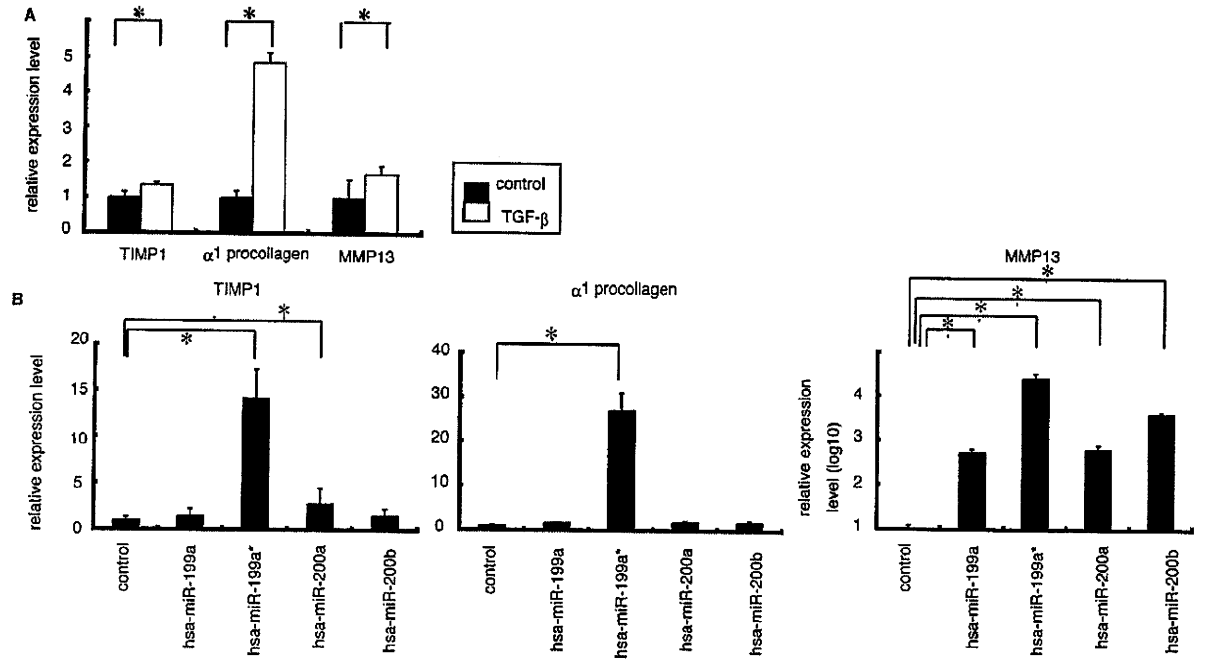

Figure 4. The relationship between expression level of miR-199 and 200 families and expression level of three fibrosis related genes. A. Administration of TGFβ in LX2 cells showed that the expression level of three fibrosis related genes were higher than that in non-treated cells. The data shown are the means+SD of three independent experiments. Asterisk was indicated to the significant difference of $p<0.05$ (two-tailed Student-t test). B. The expression levels of 3 fibrosis related genes in LX2 cells with overexpressing miR-199a, 199a*, 200a, or 200b, respectively were significantly higher than that in cells transfected with control miRNA ($p<0.05$; two-tailed Student t-test).
doi:10.1371/journal.pone.0016081.g004

Moreover miRNA expression profiling has further applications in novel anti-fibrosis therapy in CH.

Materials and Methods

Sample preparation

105 liver tissues samples from chronic hepatitis C patients (genotype 1b) were obtained by fine needle biopsy (Table S1). METAVIR fibrosis stages were F0 in 7 patients, F1 in 57, F2 in 24 and F3 in 17. Patients with autoimmune hepatitis or alcoholic liver injury were excluded. None of the patients were positive for hepatitis B virus associated antigen/ antibody or anti human immunodeficiency virus antibody. No patient received interferon therapy or immunomodulatory therapy prior to the enrollment in this study. We also obtained normal liver tissue from the Liver Transplantation Unit of Kyoto University. All of the patients or their guardians provided written informed consent, and Kyoto University Graduate School and Faculty of Medicine's Ethics Committee approved all aspects of this study in accordance with the Helsinki Declaration.

RNA preparation and miRNA microarray

Total RNA from cell lines or tissue samples was prepared using a *mir*Vana miRNA extraction Kit (Ambion, Austin, TX, USA) according to the manufacturer's instruction. miRNA microarrays were manufactured by Agilent Technologies (Santa Clara, CA, USA) and 100 ng of total RNA was labeled and hybridized using the Human microRNA Microarray Kit protocol for use with Agilent microRNA microarrays Version 1.5 and Mouse microRNA Microarray Kit protocol for use with Agilent microRNA microarrays Version 1.0. Hybridization signals were detected with a DNA microarray scanner G2505B (Agilent Technologies) and the scanned images were analyzed using Agilent feature extraction software (v9.5.3.1). Data were analyzed using GeneSpring GX 7.3.1 software (Agilent Technologies) and normalized as follows: (i) Values below 0.01 were set to 0.01. (ii) In order to compare between one-color expression profile, each measurement was divided by the 75th percentile of all measurements from the same species. The data presented in this manuscript have been deposited in NCBI's Gene Expression Omnibus and are accessible through GEO Series accession number GSE16922 (human) and accession number GSE19865 (mouse).

Real-time qPCR for human miRNA

For detection of the miRNA level by real-time qPCR, TaqMan® microRNA assay (Applied Biosystems) was used to quantify the relative expression level of miR-199a (assay ID. 002304), miR-199a* (assay ID. 000499), miR-200a (assay ID. 000502), miR-200b (assay ID. 002251), and U18 (assay ID. 001204) was used as an internal control. cDNA was synthesized using the Taqman miRNA RT Kit (Applied Biosystems). Total RNA (10 ng/ml) in 5ml of nuclease free water was added to 3 ml of 5× RT primer, 10× 1.5μl of reverse transcriptase buffer, 0.15 μl of 100 mM dNTP, 0.19 μl of RNase inhibitor, 4.16 μl of nuclease free water, and 50U of reverse transcriptase in a total volume of 15 μl. The reaction was performed for 30 min at 16°C, 30 min at 42°C, and 5 min at 85°C. All reactions were run in triplicate. Chromo 4 detector (BIO-RAD) was used to detect miRNA expression.

Animal and Chronic Mouse Liver Injury Model

Each 5 adult (8-week-old) male C57BL/6J mice were given a biweekly intra-peritoneal dose of a 10% solution of CCL_4 in olive oil (0.02 ml/g/ mouse) for the first 4 weeks and then once a week

for the next 4 weeks. At week 4, 6 or 8, the mice were sacrificed. Partial livers were fixed, embedded in paraffin, and processed for histology. Serial liver sections were stained with hematoxylin-eosin, Azan staining, Silver (Ag) staining, and Elastica van Gieson (EVG) staining, respectively. Total RNA from mice liver tissue was prepared as described previously. All animal procedures concerning the analysis of liver injury were performed in following the guidelines of the Kyoto University Animal Research Committee and were approved by the Ethical Committee of the Faculty of Medicine, Kyoto University.

Cell lines and Cell preparation

The human stellate cell lines LX-2, was provided by Scott L. Friedman. LX-2 cells, which viable in serum free media and have high transfectability, were established from human HSC lines [26]. LX-2 cells were maintained in D-MEM (Invitrogen, Carlsbad, CA, USA) with 10% fetal bovine serum, plated in 60 mm diameter dishes and cultured to 70% confluence. Huh-7 and Hela cells were also maintained in D-MEM with 10% fetal bovine serum. HuS-E/2 immortalized hepatocytes were cultured as described previously [27]. LX-2 cells were then cultured in D-MEM without serum with 0.2% BSA for 48 hours prior to TGFβ1 (Sigma-Aldrich, Suffolk, UK) treatment (2.5 ng/ml for 20 hours). Control cells were cultured in D-MEM without fetal bovine serum.

miRNA transfection

LX-2 cells were plated in 6-well plates the day before transfection and grown to 70% confluence. Cells were transfected with 50 pmol of Silencer® negative control siRNA (Ambion) or double-stranded mature miRNA (Hokkaido System Science, Sapporo, Japan) using lipofectamine RNAiMAX (Invitrogen). Cells were harvested 2 days after transfection.

Real-time qPCR

cDNA was synthesized using the Transcriptor High Fiderity cDNA synthesis Kit (Roche, Basel, Switzerland). Total RNA (2 μg) in 10.4 μl of nuclease free water was added to 1 μl of 50mM random hexamer. The denaturing reaction was performed for 10min at 65°C. The denatured RNA mixture was added to 4 μl of 5× reverse transcriptase buffer, 2 μl of 10 mM dNTP, 0.5 μl of 40U/μl RNase inhibitor, and 1.1 μl of reverse transcriptase (FastStart Universal SYBR Green Master (Roche) in a total volume of 20 μl. The reaction ran for 30 min at 50°C (cDNA synthesis), and five min at 85°C (enzyme denaturation). All reactions were run in triplicate. Chromo 4 detector (BIO-RAD, Hercules, CA, USA) was used to detect mRNA expression. The primer sequences are follows; MMP13 s; 5′-gaggctccgagaaatgcagt-3′, as; 5′-atgccatcgtgaagtctggt-3′, TIMP1 s; 5′-cttggcttctgcactgatgg-3′, as; 5′-acgctggtataaggtggtct-3′, α1-procollagen s; 5′-aacatgaccaaaaaccaaaagtg-3′, as; 5′-cattgtttcctgtgtcttctgg-3′, and β-actin s; 5′-ccactggcatcgtgatggac-3′, as; 5′-tcattgccaatggtgatgacct-3′. Assays were performed in triplicate, and the expression levels of target genes were normalized to expression of the β-actin gene, as quantified using real-time qPCR as internal controls.

Statistical analyses

Statistical analyses were performed using Student's *t*-test; *p* values less than 0.05 were considered statistically significant. Microarray data were also statistically analyzed using Welch's test and Bonferroni correction for multiple hypotheses testing.

Supporting Information

Figure S1 Time line of the induction of chronic liver fibrosis. Upward arrow indicated administration of olive oil or CCl_4. Downward arrow indicates when mice were sacrificed.
(TIF)

Figure S2 Comparison of the expression level of miR-199 and 200 familes in several cell lines and human liver tissue. Endogenous expression level of miR-199a, 199a*, 200a, and 200b in normal liver and LX2 cell as determined by microarray analysis (Agilent Technologies). Endogenous expression level of same miRNAs in Hela, Huh-7 and, immortalized hepatocyte: HuS-E/2 by previously analyzed data [9].
(TIF)

Table S1 Clinical characteristics of patients by the grade of fibrosis.
(DOCX)

Table S2 Extracted human miRNAs related to liver fibrosis.
(DOCX)

Table S3 Corresponding human and mouse miRNAs.
(DOCX)

Table S4 Hypothetical miRNA target genes according to in silico analysis.
(DOCX)

Author Contributions

Conceived and designed the experiments: YM KS. Performed the experiments: YM HT YH NK. Analyzed the data: MT MK. Contributed reagents/materials/analysis tools: YM HT YH NK. Wrote the paper: YM MT AT FM NK TO.

References

1. Wasley A, Alter MJ (2000) Epidemiology of hepatitis C: geographic differences and temporal trends. Semin Liver Dis 20: 1–16.
2. Shepard CW, Finelli L, Alter MJ (2005) Global epidemiology of hepatitis C virus infection. Lancet Infect Dis 5: 558–567.
3. Gressner AM, Weiskirchen R (2006) Modern pathogenetic concepts of liver fibrosis suggest stellate cells and TGF-beta as major players and therapeutic targets. J Cell Mol Med 10: 76–99.
4. Nilsen TW (2007) Mechanisms of microRNA-mediated gene regulation in animal cells. Trends Genet 23: 243–249.
5. Zamore PD, Haley B (2005) Ribo-gnome: the big world of small RNAs. Science 309: 1519–1524.
6. Pillai RS (2005) MicroRNA function: multiple mechanisms for a tiny RNA? Rna 11: 1753–1761.
7. Ura S, Honda M, Yamashita T, Ueda T, Takatori H, et al. (2009) Differential microRNA expression between hepatitis B and hepatitis C leading disease progression to hepatocellular carcinoma. Hepatology 49: 1098–1112.
8. Yamamoto Y, Kosaka N, Tanaka M, Koizumi F, Kanai Y, et al. (2009) MicroRNA-500 as a potential diagnostic marker for hepatocellular carcinoma. Biomarkers 14: 529–538.
9. Murakami Y, Yasuda T, Saigo K, Urashima T, Toyoda H, et al. (2006) Comprehensive analysis of microRNA expression patterns in hepatocellular carcinoma and non-tumorous tissues. Oncogene 25: 2537–2545.
10. Jin X, Ye YF, Chen SH, Yu CH, Liu J, et al. (2008) MicroRNA expression pattern in different stages of nonalcoholic fatty liver disease. Dig Liver Dis.
11. Ogawa T, Iizuka M, Sekiya Y, Yoshizato K, Ikeda K, et al. (2009) Suppression of type I collagen production by microRNA-29b in cultured human stellate cells. Biochem Biophys Res Commun.
12. Ji J, Zhang J, Huang G, Qian J, Wang X, et al. (2009) Over-expressed microRNA-27a and 27b influence fat accumulation and cell proliferation during rat hepatic stellate cell activation. FEBS Lett 583: 759–766.
13. Wienholds E, Kloosterman WP, Miska E, Alvarez-Saavedra E, Berezikov E, et al. (2005) MicroRNA expression in zebrafish embryonic development. Science 309: 310–311.

14. Landgraf P, Rusu M, Sheridan R, Sewer A, Iovino N, et al. (2007) A mammalian microRNA expression atlas based on small RNA library sequencing. Cell 129: 1401–1414.
15. Friedman SL (2008) Hepatic fibrosis-Overview. Toxicology.
16. Roderburg C, Urban GW, Bettermann K, Vucur M, Zimmermann H, et al. (2010) Micro-RNA profiling reveals a role for miR-29 in human and murine liver fibrosis. Hepatology.
17. Venugopal SK, Jiang J, Kim TH, Li Y, Wang SS, et al. (2010) Liver fibrosis causes downregulation of miRNA-150 and miRNA-194 in hepatic stellate cells, and their overexpression causes decreased stellate cell activation. Am J Physiol Gastrointest Liver Physiol 298: G101–106.
18. Jiang J, Gusev Y, Aderca I, Mettler TA, Nagorney DM, et al. (2008) Association of MicroRNA expression in hepatocellular carcinomas with hepatitis infection, cirrhosis, and patient survival. Clin Cancer Res 14: 419–427.
19. Jiang X, Tsitsiou E, Herrick SE, Lindsay MA (2010) MicroRNAs and the regulation of fibrosis. Febs J 277: 2015–2021.
20. Marquez RT, Bandyopadhyay S, Wendlandt EB, Keck K, Hoffer BA, et al. (2010) Correlation between microRNA expression levels and clinical parameters associated with chronic hepatitis C viral infection in humans. Lab Invest.
21. Kim S, Lee UJ, Kim MN, Lee EJ, Kim JY, et al. (2008) MicroRNA miR-199a* regulates the MET proto-oncogene and the downstream extracellular signal-regulated kinase 2 (ERK2). J Biol Chem 283: 18158–18166.
22. Murakami Y, Aly HH, Tajima A, Inoue I, Shimotohno K (2009) Regulation of the hepatitis C virus genome replication by miR-199a. J Hepatol 50: 453–460.
23. Gibbons DL, Lin W, Creighton CJ, Rizvi ZH, Gregory PA, et al. (2009) Contextual extracellular cues promote tumor cell EMT and metastasis by regulating miR-200 family expression. Genes Dev 23: 2140–2151.
24. Gregory PA, Bert AG, Paterson EL, Barry SC, Tsykin A, et al. (2008) The miR-200 family and miR-205 regulate epithelial to mesenchymal transition by targeting ZEB1 and SIP1. Nat Cell Biol 10: 593–601.
25. Oberti F, Valsesia E, Pilette C, Rousselet MC, Bedossa P, et al. (1997) Noninvasive diagnosis of hepatic fibrosis or cirrhosis. Gastroenterology 113: 1609–1616.
26. Xu L, Hui AY, Albanis E, Arthur MJ, O'Byrne SM, et al. (2005) Human hepatic stellate cell lines, LX-1 and LX-2: new tools for analysis of hepatic fibrosis. Gut 54: 142–151.
27. Aly HH, Watashi K, Hijikata M, Kaneko H, Takada Y, et al. (2007) Serum-derived hepatitis C virus infectivity in interferon regulatory factor-7-suppressed human primary hepatocytes. J Hepatol 46: 26–36.

Murakami et al. BMC Medical Genomics 2010, 3:48
http://www.biomedcentral.com/1755-8794/3/48

BMC Medical Genomics

RESEARCH ARTICLE Open Access

Hepatic microRNA expression is associated with the response to interferon treatment of chronic hepatitis C

Yoshiki Murakami[1*], Masami Tanaka[2], Hidenori Toyoda[3], Katsuyuki Hayashi[4], Masahiko Kuroda[2], Atsushi Tajima[5], Kunitada Shimotohno[6]

Abstract

Background: HCV infection frequently induces chronic liver diseases. The current standard treatment for chronic hepatitis (CH) C combines pegylated interferon (IFN) and ribavirin, and is less than ideal due to undesirable effects. MicroRNAs (miRNAs) are endogenous small non-coding RNAs that control gene expression by degrading or suppressing the translation of target mRNAs. In this study we administered the standard combination treatment to CHC patients. We then examined their miRNA expression profiles in order to identify the miRNAs that were associated with each patient's drug response.

Methods: 99 CHC patients with no anti-viral therapy history were enrolled. The expression level of 470 mature miRNAs found their biopsy specimen, obtained prior to the combination therapy, were quantified using microarray analysis. The miRNA expression pattern was classified based on the final virological response to the combination therapy. Monte Carlo Cross Validation (MCCV) was used to validate the outcome of the prediction based on the miRNA expression profile.

Results: We found that the expression level of 9 miRNAs were significantly different in the sustained virological response (SVR) and non-responder (NR) groups. MCCV revealed an accuracy, sensitivity, and specificity of 70.5%, 76.5% and 63.3% in SVR and non-SVR and 70.0%, 67.5%, and 73.7% in relapse (R) and NR, respectively.

Conclusions: The hepatic miRNA expression pattern that exists in CHC patients before combination therapy is associated with their therapeutic outcome. This information can be utilized as a novel biomarker to predict drug response and can also be applied to developing novel anti-viral therapy for CHC patients.

Background

Hepatitis C virus (HCV) infection affects more than 3% of the world population. HCV infection frequently induces chronic liver diseases ranging from chronic hepatitis (CH) C, to liver cirrhosis (LC) and hepatocellular carcinoma (HCC) [1]. The current standard treatment for CHC combines pegylated interferon (Peg-IFN) and ribavirin, and has been found to be effective in only 50% of HCV genotype 1b infection. Furthermore this form of therapy is often accompanied by adverse effects; therefore, there is a pressing need to develop alternative strategies to treat CHC and to identify patients that will not be responsive to treatment [2].

MicroRNAs (miRNAs) are endogenous small non-coding RNAs that control gene expression by degrading or suppressing the translation of target mRNAs [3,4]. There are currently 940 identifiable human miRNAs (The miRBase Sequence Database – Release 15.0). These miRNAs can recognize hundreds of target genes with incomplete complementary over one third of human genes appear to be conserved miRNA targets [5,6]. miRNA can associate not only several pathophysiologic events but also cell proliferation and differentiation.

However, there are many miRNAs whose functions are still unclear. Examples include miR-122 which is an abundant liver-specific miRNA that is said to constitute

* Correspondence: ymurakami@genome.med.kyoto-u.ac.jp
[1]Center for Genomic Medicine, Kyoto University Graduate School of Medicine, 53 Shogoinkawahara-cho, Sakyo-ku, Kyoto 606-8507, Japan
Full list of author information is available at the end of the article

up to 70% of all miRNA molecules in hepatocytes [7]. The expression level of miR-122 was reportedly associated with early response to IFN treatment, while others like miR-26 have expression status that is associated with HCC survival and response to adjuvant therapy with IFN [8,9]. IFN beta (IFNβ) on the other hand, has been shown to rapidly modulate the expression of numerous cellular miRNAs, and it has been demonstrated that 8 IFNβ-induced miRNAs have sequence-predicted targets within the hepatitis C virus (HCV) genomic RNA [10]. Finally several miRNAs have been recognized as having target sites in the HCV genome that inhibits viral replication [10-12].

To date, various parameters have been examined in an attempt to confirm the effects of the IFN-related treatment for CHC. In patients with chronic HCV genotype 1b infection, there is a substantial correlation between responses to IFN and mutation in the interferon sensitivity determining region (ISDR) of the viral genome [13]. Substitutions of amino acid in the HCV core region (aa 70 and aa 91) were identified as predictors of early HCV-RNA negativity and several virological responses, including sustained response to standard combination therapy [14]. In order to assess the drug response to combination therapy for CHC using gene expression signatures, several researchers cataloged the IFN related gene expression profile from liver tissue or peripheral blood mononuclear cells (PBMC) [15,16]. It was found that failed combination therapy was associated with up-regulation of a specific set of IFN-responsive genes in the liver before treatment [17]. Additional reports have indicated that two SNPs near the gene IL28B on chromosome 19 may also be associated with a patient's lack of response to combination therapy [18]. These reports suggest that gene expression during the early phase of anti-HCV therapy may elucidate important molecular pathways for achieving virological response [19].

Our aim in this study was to identify gene related factors that contribute to poor treatment response to combination therapy for CHC. In order to achieve this we studied the miRNA expression profile of CHC patients before treatment with CHC combination therapy and tried to determine the miRNAs that were associated with their drug response. Knowing patients' expression profile is expected to provide a clearer understanding of how aberrant expression of miRNAs can contribute to the development of chronic liver disease as well as aid in the development of more effective and safer therapeutic strategies for CHC.

Methods

Patients and sample preparation

Ninety-nine CHC patients with HCV genotype 1b were enrolled (Table 1). Patients with autoimmune hepatitis, or alcohol-induced liver injury, or hepatitis B virus-associated antigen/antibody or anti-human immunodeficiency virus antibody were excluded. There were no patients who received IFN therapy or immunomodulatory therapy before enrollment in the study. Serum HCV RNA was quantified before IFN treatment using Amplicor-HCV Monitor Assay (Roche Molecular Diagnostics Co., Tokyo, Japan). Liver biopsy specimen was collected from each patient up to one week prior to administering combination therapy. Histological grading and staging of liver biopsy specimens from the CHC patients were performed according to the Metavir classification system. Pretreatment blood tests were conducted to determine each patient's level of aspartate aminotransferase, alanine aminotransferase, total bilirubin, alkaline phosphatase, gamma-glutamyl transpeptidase, white blood cell (WBC), platelets, and hemoglobin. Written informed consent was obtained from all of the patients or their guardians and provided to the Ethics Committee of the Graduate School of Kyoto University, who approved the conduct of this study in accordance with the Helsinki Declaration.

Table 1 Clinical characteristics of patients

Characteristics	SVR (n = 46)	R (n = 28)	NR (n = 25)	p-value
Age (years)	57.0 ± 9.8	61.2 ± 8.3	60.6 ± 7.6	0.09†
Male (%)	28 (61%)	11 (39%)	9 (36%)	0.08§
Weight (kg)	59.5 ± 9.0	56.6 ± 9.9	56.0 ± 7.7	0.13†
HCV RNA ($\times 10^6$ copies/ml)	1.90 ± 1.95	1.83 ± 1.04	1.58 ± 0.93	0.62†
Fibrosis stage				
F 0	1	1	1	0.50§
F 1	29	16	10	
F 2	10	7	6	
F 3	6	4	7	
F 4	0	0	1	
WBC($\times 10^3/mm^3$)	5.31 ± 1.59	5.18 ± 1.24	4.71 ± 1.15	0.29†
Hemoglobin (g/dl)	14.2 ± 1.26	13.6 ± 1.35	13.5 ± 1.13	0.022†
Platelet ($\times 10^4/mm^3$)	16.7 ± 5.0	16.4 ± 4.0	15.2 ± 6.1	0.25†
AST (IU/L)	54.8 ± 48.1	46.6 ± 29.3	57.0 ± 28.5	0.17†
ALT (IU/L)	74.5 ± 87.8	47.9 ± 28.6	67.6 ± 43.2	0.15†
γGTP (IU/L)	56.0 ± 69.4	38.5 ± 28.9	74.3 ± 59.0	0.025†
ALP (IU/L)	248 ± 71.5	245 ± 75.7	323 ± 151	0.038†
Total Bilirubin (mg/dl)	0.67 ± 0.22	0.72 ± 0.30	0.68 ± 0.19	0.95†
Albumin (g/dl)	4.21 ± 0.31	4.13 ± 0.27	4.01 ± 0.48	0.14†

Abbreviations. SVR, sustained virological response; R, relapse; NR, non responder; Differences in clinical characteristics among three groups were tested using †Kruskal-Wallis test, or §Fisher's exact test. AST, aspartate aminotransferase; ALT, alanine aminotransferase; WBC, white blood cell; ALP, alkaline phosphatase; γGTP, gamma-glutamyl transpeptidase.

Treatment protocol and definitions

All enrolled patients were treated with pegylated IFNa-2b (Schering-Plough Corporation, Kenilworth, NJ, USA) and ribavirin (Schering-Plough) for 48 weeks (Figure 1). Pegylated IFN was administered at a dose of 1.5 mg kg/week at the starting point. Ribavirin was administered following the dose recommended by the manufacturer.

Definitions of drug response to therapy

Drug response was defined according to how much HCV RNA had decreased in each patient's serum. After four weeks of drug administration (rapid response phase) the patients were classified into the following two groups after four weeks of drug administration: (i) rapid virological responder (RVR): a patient whose serum was negative for serum HCV RNA at four weeks, and (ii) non-RVR: a patient who was not classified as RVR.

The patients were classified into the following three groups after 12 weeks of drug administration (early response phase): (i) complete early virological responder (cEVR): a patient who was negative for serum HCV RNA at 12 weeks; (ii) partial EVR: a patient whose serum HCV RNA was reduced by 2-log or more of the HCV RNA before drug administration at 12 weeks, but who was not negative for serum HCV RNA; and (iii) non-EVR: a patient who was not classified as either cEVR or pEVR.

The patients were classified into the following three groups at the time of post-treatment at 24 weeks (final response): (i) sustained virological responder (SVR): a patient who was negative for serum HCV RNA during the six months following completion of the combination therapy; (ii) relapse (R): a patient whose serum HCV RNA was negative by the end of the combination therapy but reappeared after completion of the combination therapy; and (iii) virological non-responder (NR): a patient who was positive for serum HCV RNA during the entire course of the combination treatment.

RNA extraction

Liver biopsy specimens were stored in RNA later (Ambion, Austin, TX, USA) at -80°C until RNA

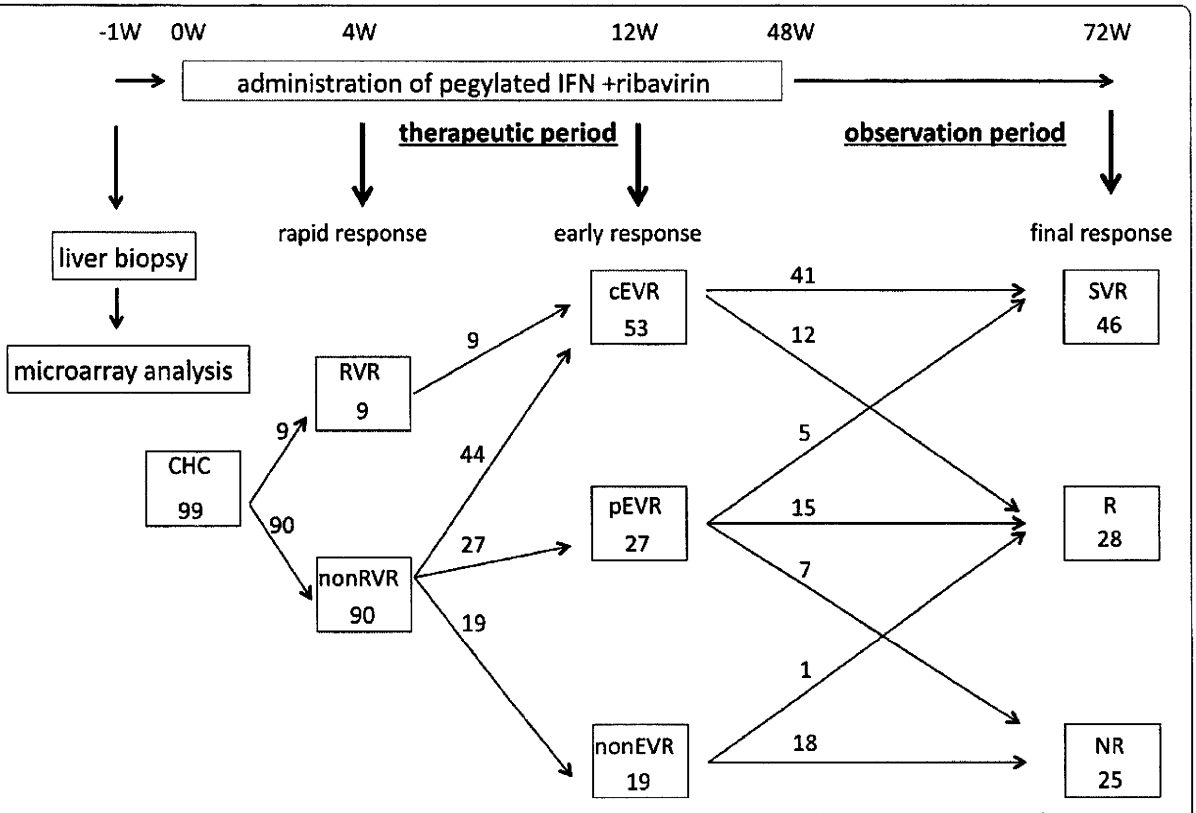

Figure 1 Study design and time-line response to combination therapy. The time-course of liver biopsy, microarray analysis, therapeutic period, observation period after combination therapy, and drug response judgment time (4W, 12W, 72W) is shown. Each therapeutic result (rapid, early, and final response) and the number of patients transitioning into each group are shown. RVR, cEVR, pEVR, SVR, R, and NR are denoted as rapid virological response, complete early virological response, partial EVR, sustained virological response, relapse, and non responder, respectively.

extraction. Total RNA was extracted by using mirVana™ miRNA Isolation kit (Ambion) according to the manufacturer's instruction.

miRNA microarray

miRNA microarrays were manufactured by using Agilent Technologies (Santa Clara, CA, USA). Total RNA (100 ng) were labeled and hybridized using a Human microRNA Microarray kit (Agilent Technologies) according to the manufacturer's protocol (Protocol for use with Agilent microRNA microarrays Version 1.5). Hybridization signals were detected using the DNA microarray scanner G2505B (Agilent Technologies), and all scanned images were analyzed using Agilent feature extraction software (v9.5.3.1). Data were analyzed using GeneSpring GX 7.3.1 software (Agilent Technologies) and normalized as follows: (i) values below 0.01 were set to 0.01. (ii) each measurement was divided by the 75th percentile of all measurements to compare one-color expression profiles. The data presented in this manuscript have been deposited in NCBI's Gene Expression Omnibus and are accessible through GEO Series accession number GSE16922: http://www.ncbi.nlm.nih.gov/geo/query/acc.cgi?token=xlmbxyyumcwkeba&acc=GSE16922

Real-time qPCR for miRNA quantification

To detect the expression level of miRNA by real-time qPCR, TaqMan® microRNA assay (Applied Biosystems) was used to quantify the relative expression levels of miR-18a (assay ID, 002422), miR-27b (assay ID, 000409), miR-422b (assay ID, 000575), miR-143 (assay ID, 000466), miR-145 (assay ID, 000467), miR-34b (assay ID, 000427), miR-378 (assay ID, 000567) and U18 (assay ID, 001204) which was used as an internal control. cDNA was synthesized by Taqman miRNA RT Kit (Applied Biosystems). Total RNA (10 ng) in 5 ul of nuclease free water was added to 3 ul of 5× RT primer, 10× 1.5 ul of reverse transcriptase buffer, 0.15 ul of 100 mM dNTP, 0.19 ul of RNase inhibitor, 4.16 ul of nuclease free water, and 50 U of reverse transcriptase in a total volume of 15 ul. The reaction was performed for 30 min at 16°C, 30 min at 42°C, and five min at 85°C. All RT reactions were run in triplicate. Chromo 4 detector (BIO-RAD, Hercules, CA, USA) was used to detect miRNA expression.

Method of predicting prognosis

Monte Carlo Cross Validation (MCCV) was used to identify a set of prognostic miRNAs and to assess and predict drug response [20,21]. We chose MCCV to make up for relatively small number of patients. The 99 enrolled patients were repeatedly and randomly divided 100 times into training sets (TSs; size n = 10, 20, ..., 90) and a corresponding validation set (VS; size = 99-n). The percentile-normalized measures for miRNA expression were compared between the 2 TS patient groups of SVR and non-SVR (R and NR) by computing absolute values of the difference for each of the 172 miRNAs that were higher than 10. A prognosis signature was defined in terms of the expression measures of the miRNAs with the largest absolute differences. A 35-miRNA prognosis predictor (PP) was established for TS patients and its performance was assessed on VS patients. A PP was computed by applying diagonal linear discriminant analysis to the 35-miRNA PP of the TS patients (Table 2 and 3). The PP was applied to predict the prognoses of the VS patients. The predicted and actual prognoses (SVR or non-SVR) of the VS patients were compared to obtain the following three measures of prognosis prediction performance: (1) accuracy (proportion of correctly predicted prognoses), (2) sensitivity (proportion of correctly predicted non-SVR) and (3) specificity (proportion of correctly predicted SVR). 53 patients (N and NR) were also repeatedly and randomly divided 100 times into training sets (TSs; size n = 6, 12, ...42) and corresponding validation set (VS; size = 53-n). Perl programs of our own writing performed all analytical processes.

Cell lines and miRNA transfection

HEK293 cells were maintained in D-MEM (Invitrogen, Carlsbad, CA, USA) with 10% fetal bovine serum, plated in 60 mm diameter dishes and cultured to 70% confluence. 293 cells were plated in 6-well plates the day before transfection and grown to 70% confluence. Cells were transfected with 50 pmol of Silencer® negative control siRNA (Ambion) or double-stranded mature miRNA (ds miRNA) or 2'-O-methylated antisense oligonucleotide against the miRNA of interest (ASO miRNA) (Hokkaido System Science, Sapporo, Japan) using lipofectamine RNAiMAX (Invitrogen). Cells were harvested 2 days after transfection.

Real-time qPCR for mRNA quanification

cDNA was synthesized using the Transcriptor High Fiderity cDNA synthesis Kit (Roche, Basel, Switzerland). Total RNA (2 μg) in 10.4 μl of nuclease free water was added to 1 μl of 50 mM random hexamer. The denaturing reaction was performed for 10 min at 65°C. The denatured RNA mixture was added to 4 μl of 5× reverse transcriptase buffer, 2 μl of 10 mM dNTP, 0.5 μl of 40 U/μl RNase inhibitor, and 1.1 μl of reverse transcriptase (FastStart Universal SYBR Green Master (Roche) in a total volume of 20 μl. The reaction ran for 30 min at 50°C (cDNA synthesis), and five min at 85°C (enzyme denaturation). All reactions were run in triplicate. Chromo 4 detector (BIO-RAD, Hercules, CA, USA) was used to detect mRNA expression. The primer sequences are as follows; BCL2 s; 5'-gttgctttacgtggcctgtt-3', as; 5'-ggaggtctggcttcatacca-3', RARA s; 5'-cataccctgccataccaacc-

Table 2 List of the 35 miRNAs used to classify patients into SVR and non-SVR groups using Monte Carlo Cross Validation (MCCV)

Gene name	fold change (SVR/non SVR)	T-test	Selection by MCCV		
			Rank	appearance frequency in this classification (%)	appearance number of times
hsa-miR-122a	1.32	6.67E-02	1	98.78	889
hsa-miR-21	1.19	3.62E-01	2	94.67	852
hsa-miR-22	1.23	7.80E-02	3	93.22	839
hsa-let-7a	1.14	3.57E-01	4	92.33	831
hsa-miR-23b	1.41	1.72E-02	5	91.44	823
hsa-miR-26a	1.32	7.45E-02	6	90.78	817
hsa-let-7f	1.15	4.04E-01	7	88.67	798
hsa-miR-142-3p	1.39	1.45E-01	8	87.33	786
hsa-miR-494	2.18	5.85E-03	9	82.00	738
hsa-miR-194	1.22	1.70E-01	10	80.78	727
hsa-let-7b	1.11	3.59E-01	11	80.22	722
hsa-miR-148a	1.25	2.28E-01	12	79.67	717
hsa-miR-29a	1.16	2.73E-01	13	77.78	700
hsa-miR-125b	1.20	2.37E-01	14	73.11	658
hsa-miR-192	1.09	4.89E-01	15	69.67	627
hsa-miR-24	1.25	8.31E-02	16	68.89	620
hsa-miR-768-3p	1.19	1.78E-01	17	68.78	619
hsa-miR-126	1.07	6.75E-01	18	49.56	446
hsa-miR-19b	1.15	2.98E-01	19	48.89	440
hsa-miR-370	2.00	1.44E-02	20	39.00	351
hsa-miR-29c	1.26	1.37E-01	21	38.89	350
hsa-miR-16	1.24	2.08E-01	22	37.11	334
hsa-miR-145	1.01	9.25E-01	23	34.89	314
hsa-let-7c	1.21	1.41E-01	24	33.22	299
hsa-miR-215	1.20	3.65E-01	25	27.67	249
hsa-let-7g	1.16	3.64E-01	26	27.44	247
hsa-miR-451	1.13	6.94E-01	27	23.11	208
hsa-miR-26b	1.30	2.26E-01	28	22.22	200
hsa-miR-92	1.12	3.44E-01	29	21.11	190
hsa-miR-29b	1.19	2.62E-01	30	19.44	175
hsa-miR-107	1.21	1.58E-01	31	18.78	169
hsa-miR-27b	1.40	2.32E-02	32	18.11	163
hsa-miR-638	1.32	5.57E-02	33	16.89	152
hsa-miR-199a*	1.12	5.92E-01	34	16.78	151
hsa-miR-193b	1.25	7.24E-02	35	16.67	150

3', as; 5'-gacatgaaaggagagtgggg-3', SMAD2 s; 5'-aatattttgg ggactgatgcc-3', as; 5'-gcttttgggcagtggttaag-3', and β-actin s; 5'-ccactggcatcgtgatggac-3', as; 5'-tcattgccaatggtgat-gacct-3'. Assays were performed in triplicate, and the expression levels of target genes were normalized to the expression of the β-actin gene, as quantified using real-time qPCR as internal controls.

Statistical analysis

Data were statistically analyzed using the Student's t-test and differences in clinical characteristics among 3 groups were tested using the Kruskal-Wallis test, or Fisher's exact test. Data from microarray were also statically analyzed using Welch's test and Benjamini-Hochberg correction for multiple hypotheses testing.

Results

A microarray platform was used to determine miRNA expression of 470 miRNAs in 99 fresh-frozen CHC liver tissues.

miRNAs which related to the final response of combination therapy

Unique miRNA expression patterns were established according to the final virological response (SVR, R, and NR) to the combination therapy (Figure 1). To isolate

Table 3 List of the miRNAs used to classify patients into R and NR groups

Gene name	fold change (R/NR)	T-test	Selection by MCCV		
			Rank	appearance frequency in this classification (%)	appearance number of times
hsa-miR-122a	1.50	6.70E-02	1	98.57	690
hsa-miR-21	1.13	5.43E-01	2	89.86	629
hsa-let-7a	1.15	4.23E-01	3	88.71	621
hsa-let-7f	1.24	3.01E-01	4	87.43	612
hsa-miR-148a	1.70	4.51E-02	5	82.71	579
hsa-miR-192	1.24	1.93E-01	6	81.71	572
hsa-miR-126	1.21	3.19E-01	7	74.14	519
hsa-miR-22	1.04	7.88E-01	8	68.43	479
hsa-miR-194	1.20	3.63E-01	9	64.29	450
hsa-miR-23b	1.30	2.06E-01	10	62.00	434
hsa-miR-125b	1.23	2.88E-01	11	61.86	433
hsa-miR-494	0.45	8.17E-02	12	61.14	428
hsa-miR-19b	1.17	3.86E-01	13	61.14	428
hsa-miR-29a	1.11	5.44E-01	14	59.86	419
hsa-miR-26a	1.13	5.38E-01	15	58.43	409
hsa-let-7b	1.01	9.37E-01	16	56.86	398
hsa-miR-142-3p	1.15	5.54E-01	17	52.71	369
hsa-miR-215	1.28	3.93E-01	18	52.00	364
hsa-miR-101	1.31	1.26E-01	19	49.00	343
hsa-miR-451	1.35	5.25E-01	20	48.14	337
hsa-miR-145	0.99	9.76E-01	21	47.14	330
hsa-let-7g	1.15	4.84E-01	22	44.00	308
hsa-miR-29c	1.23	2.94E-01	23	43.71	306
hsa-miR-26b	1.37	2.85E-01	24	43.14	302
hsa-miR-768-3p	1.00	9.91E-01	25	36.29	254
hsa-let-7c	1.16	3.76E-01	26	36.14	253
hsa-miR-370	0.43	7.36E-02	27	35.57	249
hsa-miR-92	1.07	6.65E-01	28	34.14	239
hsa-miR-16	1.11	6.18E-01	29	26.71	187
hsa-miR-29b	1.14	5.19E-01	30	25.71	180
hsa-miR-27b	1.40	1.15E-01	31	25.71	180
hsa-miR-24	1.08	6.56E-01	32	20.57	144
hsa-miR-107	1.00	9.81E-01	33	19.57	137
hsa-miR-143	0.95	7.99E-01	34	18.43	129
hsa-miR-214	0.85	3.61E-01	35	17.86	125

the miRNAs that were associated with the drug response to the combination therapy, we chose miRNAs which had ≥ 1.25 fold difference in the mean values of the gene expression level between at least two groups ($p < 0.05$). Unsupervised hierarchical clustering based on all the miRNAs spotted on the chip, revealed a marked, very distinct separation according to the patients' final response of the CHC liver tissue to the Peg-IFN and ribavirin combination therapy (Figure 2).

The result was that the expression level of 3 miRNAs (miR-27b, miR-378, miR-422b) in SVR was significantly higher than that in NR, whereas the expression level of 5 miRNAs (miR-34b, miR-145, miR-143, miR-652, and miR-18a) in SVR was significantly lower than that in NR. Without FDR correction, the expression level of miR-122 in NR was lower than that in SVR. The expression level of 2 miRNAs in SVR was significantly higher than that in R, whereas the expression level of 10 miRNAs in SVR was significantly lower than in that in R. Additionally, the expression level of miR-148a in R was significantly higher than that in NR. There was no significant difference in the expression level of miR-122 in NR and R (Table 4).

Validation of the microarray result by real-time qPCR

The three miRNAs (miR-18a, miR-27b, and miR-422b) with the smallest difference of fold change between NR and SVR groups and four miRNA (miR-143, miR-145,

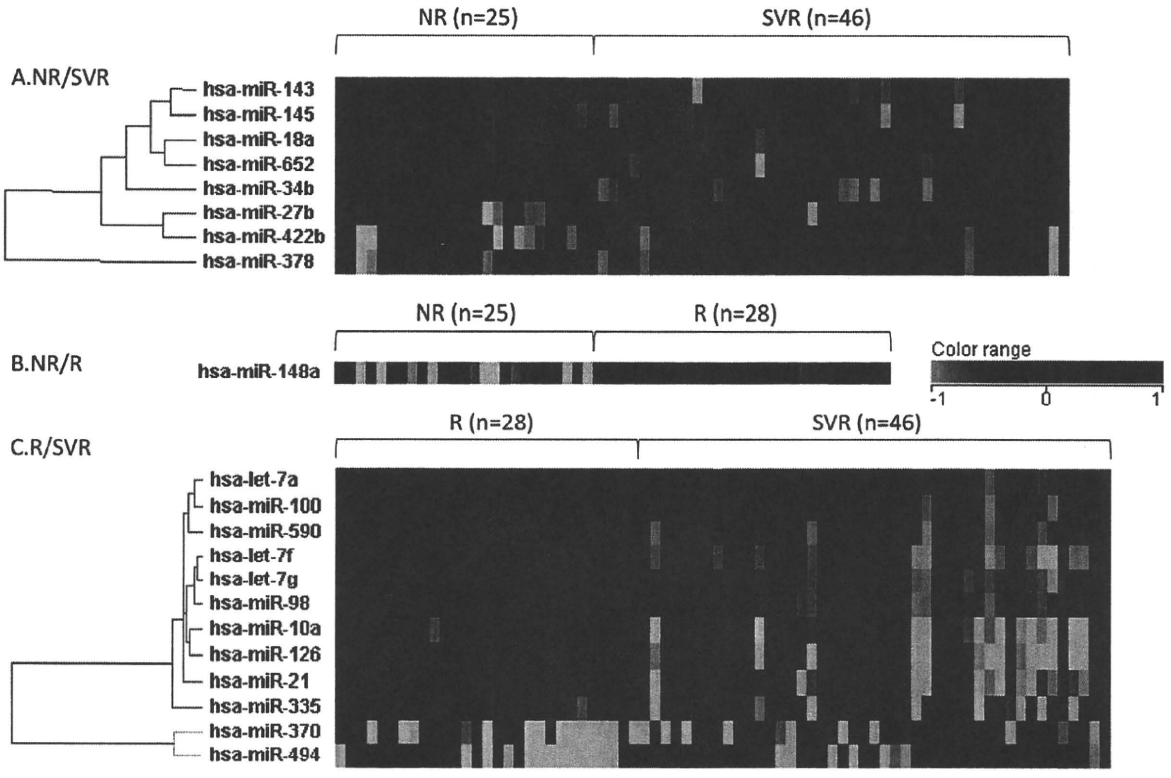

Figure 2 Clustering of CHC patients according to their final response to Peg-IFN and ribavirin combination therapy. Heatmap using miRNA differently expressed among SVR, R, and NR is shown (A: classification between NR and SVR, B: classification between NR and R, and C: classification between R and SVR, respectively). Vertical bars represent the miRNA genes and the horizontal bars represent the samples. Green bars reflect downregulated genes and red bars upregulated genes.

miR-34b, and miR-378) with the largest difference of fold change between NR and SVR groups were chosen to confirm the microarray results using stem-loop based real-time qPCR. The result of real-time qPCR corresponded to the result from the microarray analysis (Figure 3).

miRNAs which related to the 4 week (rapid response phase) response to combination therapy

The miRNA expression profile was established according to the rapid phase response to the combination therapy by week 4 (Table 5). Our results showed that the expression level of 5 miRNAs in non-RVR was significantly higher than that in RVR. Prior results have revealed that a patient who achieves RVR as a result of the combination therapy has a high possibility of achieving SVR [22,23]. Our research supports this finding: nine out of 99 patients achieved RVR. All nine cases shifted to cEVR by week 12, and 8 shifted to SVR at the final response. The 90 cases in non-RVR shifted to 44 cases in cEVR, 19 in pEVR, and 27 in non-EVR and at the final response shifted to 38 cases in SVR, 27 in R, and 25 in NR (Table 6 and Figure 1).

miRNAs which related to the 12 week (early response phase) response to combination therapy

Establishing the miRNA expression profile of patients according to their 12 week (early response) of CHC liver specimen to the combination therapy after 12 weeks, showed that the expression level of miR-23b and miR-422b in cEVR was higher than that in non-EVR, and the expression level of miR-34b in cEVR lower than that in non-EVR (Table 5). There were no miRNAs with expression level that differed significantly between cEVR and pEVR, and non-EVR and pEVR. The drug response at 12 weeks appeared to be a predictive factor of the final drug response. The 53 cases in cEVR at week 12 shifted to 41 cases in SVR and 12 in R at the final response. 27 cases in pEVR at week 12, shifted to 5 in SVR, 15 in R, and 7 in NR and 19 in non-EVR shifted to 1 in R and 18 in NR (Table 6 and Figure 1).

Predicting the final outcome before drug administration using MCCV

Before initial drug administration, we attempted to simulate the clinical outcome of the combination

Table 4 Extracted miRNA related to the final outcome of combination therapy

Gene Name	Fold Change (NR/SVR)	p-value with FDR correction	p-value without correction
hsa-miR-34b*	1.50	3.53E-02	6.95E-05
hsa-miR-145	1.35	3.55E-02	5.50E-05
hsa-miR-143	1.31	4.65E-02	6.46E-04
hsa-miR-652	1.28	4.33E-02	3.43E-04
hsa-miR-18a	1.22	4.33E-02	2.02E-05
hsa-miR-27b	0.78	4.33E-02	3.97E-05
hsa-miR-422b*	0.71	4.33E-02	1.44E-04
hsa-miR-378	0.70	4.86E-02	1.38E-03
hsa-miR-122	0.72	> 5.00E-02	2.59E-04

Gene Name	Fold Change (NR/R)	p-value with FDR correction	p-value without correction
hsa-miR-148a	0.59	1.60E-02	8.99E-04
has-miR-122	0.72	> 5.00E-02	6.23E-04

Gene Name	Fold Change (R/SVR)	P-value	p-value without correction
hsa-let-7a	1.15	3.93E-02	1.94E-03
hsa-let-7f	1.24	1.04E-02	3.60E-03
hsa-let-7g	1.17	1.93E-02	1.82E-02
hsa-miR-100	1.23	1.93E-02	9.23E-04
hsa-miR-10a	1.37	1.26E-02	2.40E-03
hsa-miR-126	1.36	1.04E-02	1.50E-03
hsa-miR-21	1.30	4.78E-02	3.45E-02
hsa-miR-335	2.00	2.83E-02	3.50E-02
hsa-miR-370	0.36	1.38E-02	2.96E-03
hsa-miR-494	0.37	3.93E-02	1.97E-03
hsa-miR-590	1.26	3.93E-02	5.59E-03
hsa-miR-98	1.22	1.38E-02	6.64E-03

Asterisk was denoted the common miRNAs appeared whose expression level between NR and SVR, and nonEVR and cEVR.

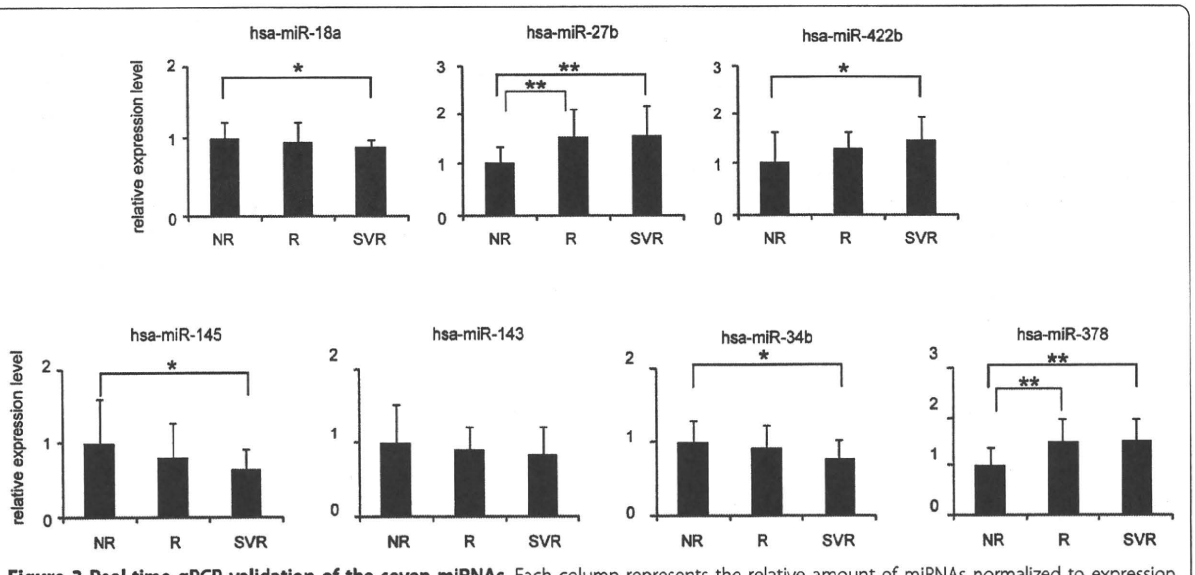

Figure 3 Real-time qPCR validation of the seven miRNAs. Each column represents the relative amount of miRNAs normalized to expression level of U18. The data shown were means+SD of three independent experiments. Asterisk indicates a significant difference of $p < 0.05$ (*) or $p < 0.01$ (**).

Table 5 List of the miRNA related to the rapid or early outcome of combination therapy

Gene Name	Fold Change (non RVR/RVR)	p-value	p-value without correction
hsa-let-7c	1.17	2.01E-02	8.31E-03
hsa-let-7d	1.13	3.50E-02	5.63E-02
hsa-miR-139	1.29	3.35E-02	2.70E-02
hsa-miR-324-5p	1.14	1.64E-02	3.24E-02
hsa-miR-768-5p	1.34	4.57E-02	1.29E-02

Gene Name	Fold Change (non EVR/cEVR)	p-value	p-value without correction
hsa-miR-34b*	1.51	3.30E-02	1.69E-04
hsa-miR-23b	0.74	2.69E-02	8.91E-05
hsa-miR-422b*	0.67	2.40E-02	1.34E-04
hsa-miR-122	0.74	> 5.00E-02	3.07E-03

Asterisk was denoted the common miRNAs appeared whose expression level between NR and SVR, and nonEVR and cEVR.

therapy before drug administration by using MCCV. We first extracted the SVR and non-SVR groups from all of the patients, and then the R and NR groups were predicted afterwards. MCCV simulation showed that the accuracy, specificity, and sensitivity of the liver specimen classified as SVR or non-SVR was up to 70.5%, 63.3%, and 76.8%, respectively (TSs = 80). On the other hand, the accuracy, specificity, and sensitivity of the liver specimen classified as R or NR was 70.0%, 73.7%, and 67.5%, respectively (TSs = 42)(Figure 4). Fold change of their normalized expression level, P value, and number of selection by MCCV in the 35 informative miRNAs that were identified based on the all patients are shown in Table 2 and 3.

miRNAs related to the final drug response can regulate the immune related genes

In order to clarify the biological links between miRNAs and IFN responses, we examined whether the expression of immune-related hypothetical miRNAs target genes (additional file 1) could be controlled by miRNAs which were related to the final drug response. We observed the changes in expression level of B-cell CLL/lymphoma 2 (BCL2), retinoic acid receptor, alpha (RARA), and SMAD family member 2 (SMAD2) by real-time qRT-PCR as the expression level of miRNAs (miR-143, miR-27b, and miR-18a) was modified, respectively, in HEK293 cells. The expression level of the hypothetical targets examined was down-regulated by over-expression of the corresponding miRNA and the corresponding antisense oligonucleotide (ASO) inhibited the function of miRNA (additional file 2).

Discussion

Our large and comprehensive screening revealed that hepatic miRNA expression can be associated with a patient's drug response. There are several reports that miRNAs are closely related to innate immunity, and in this study, we found that several miRNAs had the potential to recognize immuno-related genes as target candidates [24-26]. For example, the following hypothetical candidate genes of miR-378, miR-18a, miR-27b, miR-34b, and miR-145 each identified as target genes, Interferon Response Factor (IRF) 1, IRF2, IRF4, IRF6, and IRF7, respectively (additional file 1). Past reports show that miR-422b was related to the B cell differentiation [27]. When an immuno-reaction induces aberrant expression of miRNA, the expression level of miR-34b significantly decreased in H69 cells following IFN-γ stimulation [28]. Bcl-6 positively directs follicular helper T cell differentiation, through combined repression of miR-18a and miR-27b and transcription factors [29].

In our study, there was significant difference in the fold change of the expression level of miRNA based on the drug response, however, the absolute value of the fold change was not so significant (Table 4). Usually one miRNA can regulate many genes including immuno-related gene (additional file 1), and these genes in turn can synergistically affect immune activity. In our preliminary study (additional file 2) BCL-2, RARA, and SMAD2 can be regulated by miR-143, miR-18a, and miR-27b, respectively. Considering that the expression level of several miRNAs changed these minute changes taken together can have a significant impact on a patient's drug-response and innate immunity.

Aberrant expression of miRNA can modify the replication of HCV. According to Vita algorithm, several miRNAs, related to drug response, can recognize HCV genotype 1b sequence as a target (additional file 3) [30]. For example, miR-199a* is able to target the HCV genome and inhibit viral replication [12]. IFN has the ability to modulate expression of certain miRNAs that may either target the HCV RNA genome (miR-196 or miR-

Table 6 Patients' periodical drug response changes

code No.	4W treatment (rapid response)	12W treatment (early response)	48W treatment +24W observation (final outcome)	code No	4W treatment (rapid response)	12W treatment (early response)	48W treatment +24W observation (final outcome)
OCH-105	non RVR	non EVR	NR	OCH-103	RVR	cEVR	SVR
OCH-111	non RVR	pEVR	NR	OCH-104	non RVR	cEVR	SVR
OCH-118	non RVR	non EVR	NR	OCH-107	non RVR	cEVR	SVR
OCH-119	non RVR	non EVR	NR	OCH-108	non RVR	cEVR	SVR
OCH-122	non RVR	pEVR	NR	OCH-109	non RVR	cEVR	SVR
OCH-123	non RVR	non EVR	NR	OCH-110	non RVR	cEVR	SVR
OCH-126	non RVR	non EVR	NR	OCH-112	non RVR	pEVR	SVR
OCH-127	non RVR	non EVR	NR	OCH-114	RVR	cEVR	SVR
OCH-132	non RVR	pEVR	NR	OCH-116	non RVR	cEVR	SVR
OCH-137	non RVR	non EVR	NR	OCH-121	non RVR	pEVR	SVR
OCH-140	non RVR	pEVR	NR	OCH-124	non RVR	cEVR	SVR
OCH-142	non RVR	non EVR	NR	OCH-130	non RVR	cEVR	SVR
OCH-144	non RVR	pEVR	NR	OCH-131	non RVR	cEVR	SVR
OCH-145	non RVR	non EVR	NR	OCH-136	non RVR	cEVR	SVR
OCH-192	non RVR	non EVR	NR	OCH-138	non RVR	cEVR	SVR
OCH-204	non RVR	non EVR	NR	OCH-139	non RVR	cEVR	SVR
OCH-205	non RVR	non EVR	NR	OCH-143	non RVR	cEVR	SVR
OCH-206	non RVR	non EVR	NR	OCH-150	non RVR	cEVR	SVR
OCH-207	non RVR	non EVR	NR	OCH-153	non RVR	cEVR	SVR
OCH-208	non RVR	non EVR	NR	OCH-154	non RVR	cEVR	SVR
OCH-209	non RVR	pEVR	NR	OCH-155	non RVR	cEVR	SVR
OCH-210	non RVR	non EVR	NR	OCH-156	non RVR	cEVR	SVR
OCH-211	non RVR	non EVR	NR	OCH-157	non RVR	pEVR	SVR
OCH-223	non RVR	non EVR	NR	OCH-158	non RVR	pEVR	SVR
OCH-242	non RVR	pEVR	NR	OCH-160	non RVR	cEVR	SVR
OCH-101	non RVR	cEVR	R	OCH-186	non RVR	cEVR	SVR
OCH-102	RVR	cEVR	R	OCH-187	non RVR	cEVR	SVR
OCH-106	non RVR	non EVR	R	OCH-189	non RVR	pEVR	SVR
OCH-113	non RVR	pEVR	R	OCH-190	non RVR	cEVR	SVR
OCH-115	non RVR	cEVR	R	OCH-191	RVR	cEVR	SVR
OCH-117	non RVR	cEVR	R	OCH-194	non RVR	cEVR	SVR
OCH-120	non RVR	pEVR	R	OCH-195	non RVR	cEVR	SVR
OCH-125	non RVR	pEVR	R	OCH-222	non RVR	cEVR	SVR
OCH-128	non RVR	pEVR	R	OCH-228	non RVR	cEVR	SVR
OCH-129	non RVR	pEVR	R	OCH-229	RVR	cEVR	SVR
OCH-133	non RVR	pEVR	R	OCH-230	non RVR	cEVR	SVR
OCH-134	non RVR	pEVR	R	OCH-231	non RVR	cEVR	SVR
OCH-135	non RVR	cEVR	R	OCH-232	non RVR	cEVR	SVR
OCH-141	non RVR	cEVR	R	OCH-233	non RVR	cEVR	SVR
OCH-151	non RVR	pEVR	R	OCH-234	RVR	cEVR	SVR
OCH-152	non RVR	pEVR	R	OCH-236	non RVR	cEVR	SVR
OCH-159	non RVR	pEVR	R	OCH-237	non RVR	cEVR	SVR
OCH-188	non RVR	cEVR	R	OCH-238	non RVR	cEVR	SVR
OCH-213	non RVR	cEVR	R	OCH-240	RVR	cEVR	SVR
OCH-214	non RVR	pEVR	R	OCH-241	RVR	cEVR	SVR
OCH-215	non RVR	pEVR	R	OCH-243	RVR	cEVR	SVR
OCH-216	non RVR	cEVR	R				
OCH-217	non RVR	pEVR	R				
OCH-218	non RVR	cEVR	R				

Table 6: Patients?'? periodical drug response changes *(Continued)*

OCH-219	non RVR	pEVR	R
OCH-220	non RVR	cEVR	R
OCH-221	non RVR	pEVR	R
OCH-239	non RVR	cEVR	R

448) or markedly enhance its replication (miR-122) [10,11]. The low expression level of miR-122 in the subjects shown in the NR group is in accordance with our results, however, after miRNA expression profile with FDR correction, the expression level of miR-122 was not significantly different between SVR and NR groups [8]. One reason why this difference is that their study comprised of patients infected with HCV genotype from 1 to 4 while this study consisted of HCV genotype 1b patients only.

The expression pattern of mRNA in HCV infected liver tissue is different from that of healthy tissue [15]. The expression pattern of the IFN-related genes in liver tissue before administering of IFN therapy, also differs according to the drug response [15,19]. The amount of plasmacytoid dendritic cell (pDC), which are the most potent secretors of antiviral Type-I IFN, has been shown to decrease in the peripheral blood of patients, however, pDC tend to become trapped in the liver tissue if HCV infection is present [31,32]. Taken together, it is possible that the variation in the miRNA expression pattern according to the drug response existed even before therapy.

Previously, large randomized controlled trials of IFN therapy for CHC, identified at pre-treatment stage several possible factors which are associated with the final virological response. These factors include: genotype, amount of HCV RNA in peripheral blood, degree of fibrosis, age, body weight, ethnicity, and steatosis [33]. Viral genome mutation in the ISDR region and the

A

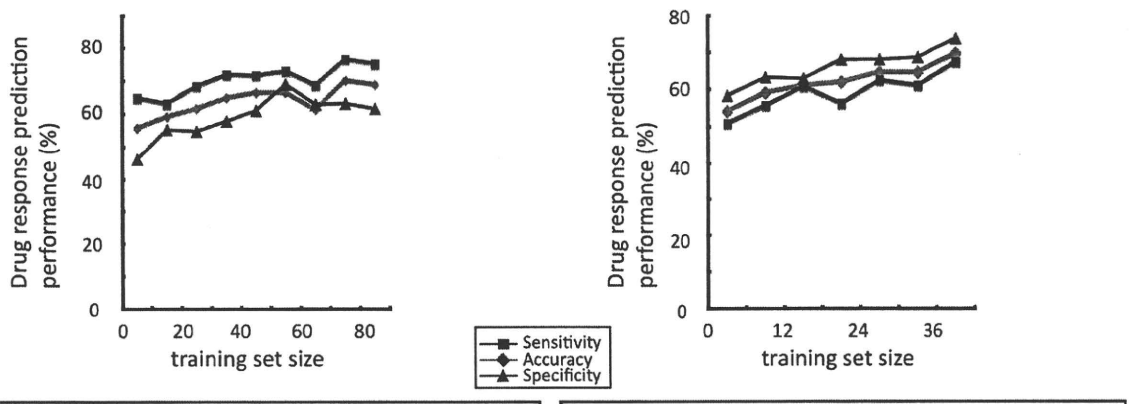

B

Training	Validation	Accuracy(%)	Sensitivity(%)	Specificity(%)	miRNA_Number
10	89	56.10	65.06	46.31	23
20	79	59.54	63.32	55.38	34
30	69	62.00	68.61	54.91	14
40	59	65.22	72.09	57.93	17
50	49	66.80	71.92	61.12	17
60	39	66.77	73.26	69.07	15
70	29	61.72	68.98	62.99	30
80	19	70.47	76.82	63.31	18
90	9	69.22	75.52	61.72	18

Training	Validation	Accuracy(%)	Sensitivity(%)	Specificity(%)	miRNA_Number
6	48	54.31	51.03	58.29	5
12	42	59.33	55.75	63.24	22
18	36	61.31	60.87	62.87	34
24	30	62.23	56.31	68.07	11
30	24	64.96	62.52	68.09	18
36	18	64.89	61.17	68.69	24
42	12	70.00	67.53	73.73	26

Figure 4 Method for predicting the clinical outcome using MCCV. Prediction performance of signatures from 35 miRNAs (Table 2 and 3). Left: Mean accuracy, specificity, and sensitivity (% in vertical axis) as a function of the training set size were determined for the 100 random splits of patients (non-SVR (NR+R) vs. SVR). Right: prediction performance of the training set size was determined by performing 48 random splits of patients (NR vs. R). A. Prediction performance (mean accuracy, specificity, and sensitivity) and number of miRNAs which was used for the prediction are also shown in each training set (TS) and validation set (VS).

substitutions of amino acid in the HCV core region also served as predictors of early, as well as end-of treatment response [13,14]. The miRNA expression obtained from the therapeutic response, can be applied to the prediction of drug response. The advantages of using miRNA for the microarray analysis include the following; (i) It was relatively easy to analyze because fewer probes were installed compared with the usual cDNA array. (ii) The change in each manifestation of a miRNA was low, in fact, in most miRNA, standard deviation was twice or less in average value (data not shown). The expression levels of miR-34b and 422b in the early response phase and final responses to treatment were consistently and significantly high and low in non-responders, respectively. Therefore these two miRNAs may be useful markers for early-to-final drug response to the IFN treatment.

Further studies are indeed needed to clarify the connection between miRNA expression and patient response to CHC combination therapy. Because information on miRNA is regularly being updated, we are planning to performed more analysis using the latest microarray and a larger sample in the future. However, in the meantime, as we have shown in Figure 4, the bigger the size of the training set, the higher the prediction performance that is achieved. This combined with the results of our Monte Carlo cross validation provided a strong based to verify the concepts in this report. We believe that our results have three advantages (i) the prediction methods used were quite reasonable, (ii) the prediction performance can later be improved if more patients' data become available and (iii) obtaining miRNA profile (not specific miRNAs) is useful for predicting the drug response. While current therapy is based on positive selection with HCV genotype or negative selection with IL28B SNP, and is limited to only some cases, our methods are applicable to all patients [13,18].

Conclusions

Our study shows that the specific miRNA are expressed differently depending on patient's drug response. As result we feel that miRNA profiling can be useful for predicting patient drug response before the administering combination therapy thereby reducing ineffective treatments. Moreover, miRNA expression profile can facilitate the accumulation of basal information for the development of novel therapeutic strategies. This approach allows for more suitable therapeutic strategies based on clinical information of individuals.

Additional material

Additional file 1: miRNA hypothetical target genes according to in silico analysis.

Additional file 2: Real-time qPCR validation of immune-related hypothetical target genes of miRNAs. The expression levels of hypothetical target genes in HEK293 cells were compared among three groups treated with control RNA, ds miRNA, and ASO miRNA. The data shown are means+SD of three independent experiments. Asterisk indicates a significant difference of $p < 0.05$.

Additional file 3: human miRNA target on the HCV genome genotype 1b (Accession No. AF333324)

List of abbreviations

HCV: hepatitis C virus; CH: chronic hepatitis C; LC: liver cirrhosis; HCC: hepatocellular carcinoma; miRNA: microRNA; IFN, interferon; SVR: sustained virological responder; R: relapse; NR: non-responder; RVR: rapid virological responder; EVR: early virological responder.

Acknowledgements

YM and KS were financially supported by the Ministry of Health, Labour and Welfare of Japan. They also received Grants-in-Aid for scientific research from the Ministry of Education, Culture, Sports, Science and Technology. MKwas financially supported by the 'Strategic Research-Based Support' Project for private universities; with matching funds from the Ministry of Education, Culture, Sports, Science and Technology.

Author details

[1]Center for Genomic Medicine, Kyoto University Graduate School of Medicine, 53 Shogoinkawahara-cho, Sakyo-ku, Kyoto 606-8507, Japan. [2]Department of Molecular Pathology, Tokyo Medical University, 6-1-1 Shinjuku, Shinjuku-ku, Tokyo 160-8402, Japan. [3]Department of Gastroenterology, Ogaki Municipal Hospital, 86-4 Minaminokawa-cho, Ogaki, Gifu 503-8502, Japan. [4]DNA Chip Research Inc., 43-1-1 Suehiro-cho, Tsurumi-ku, Yokohama, Kanagawa 230-0045, Japan. [5]Department of Molecular Life Science, Tokai University School of Medicine, 143 Shimokasuya, Isehara, Kanagawa 259-1193, Japan. [6]Research Institute, Chiba Institute for Technology, 2-17-1 Tsudanuma, Narashino, Chiba 275-0016, Japan.

Authors' contributions

YM and KS conceived and designed the experiments; YM, HT and KH performed the experiments; MT and MK performed statistical analysis; YM, MT, HT and AT contributed to writing and editing the manuscript. All authors read and approved the manuscript.

Competing interests

The authors declare that they have no competing interests.

Received: 13 June 2010 Accepted: 22 October 2010
Published: 22 October 2010

References

1. Guidotti LG, Chisari FV: **Immunobiology and pathogenesis of viral hepatitis.** *Annu Rev Pathol* 2006, 1:23-61.
2. Fried MW, Shiffman ML, Reddy KR, Smith C, Marinos G, Goncales FL, Haussinger D, Diago M, Carosi G, Dhumeaux D, Craxi A, Lin A, Hoffman J, Yu J: **Peginterferon alfa-2a plus ribavirin for chronic hepatitis C virus infection.** *N Engl J Med* 2002, **347(13)**:975-982.
3. Ambros V: **The functions of animal microRNAs.** *Nature* 2004, **431(7006)**:350-355.
4. Nilsen TW: **Mechanisms of microRNA-mediated gene regulation in animal cells.** *Trends Genet* 2007, **23(5)**:243-249.
5. Zamore PD, Haley B: **Ribo-gnome: the big world of small RNAs.** *Science (New York, NY)* 2005, **309(5740)**:1519-1524.
6. Pillai RS: **MicroRNA function: multiple mechanisms for a tiny RNA?** *RNA (New York, NY)* 2005, **11(12)**:1753-1761.
7. Lagos-Quintana M, Rauhut R, Yalcin A, Meyer J, Lendeckel W, Tuschl T: **Identification of tissue-specific microRNAs from mouse.** *Curr Biol* 2002, **12(9)**:735-739.

8. Sarasin-Filipowicz M, Krol J, Markiewicz I, Heim MH, Filipowicz W: **Decreased levels of microRNA miR-122 in individuals with hepatitis C responding poorly to interferon therapy.** *Nat Med* 2009, **15(1)**:31-33.
9. Ji J, Shi J, Budhu A, Yu Z, Forgues M, Roessler S, Ambs S, Chen Y, Meltzer PS, Croce CM, Qin LX, Man K, Lo CM, Lee J, Ng IO, Fan J, Tang ZY, Sun HC, Wang XW: **MicroRNA expression, survival, and response to interferon in liver cancer.** *N Engl J Med* 2009, **361(15)**:1437-1447.
10. Pedersen IM, Cheng G, Wieland S, Volinia S, Croce CM, Chisari FV, David M: **Interferon modulation of cellular microRNAs as an antiviral mechanism.** *Nature* 2007, **449(7164)**:919-922.
11. Jopling CL, Yi M, Lancaster AM, Lemon SM, Sarnow P: **Modulation of hepatitis C virus RNA abundance by a liver-specific MicroRNA.** *Science (New York, NY)* 2005, **309(5740)**:1577-1581.
12. Murakami Y, Aly HH, Tajima A, Inoue I, Shimotohno K: **Regulation of the hepatitis C virus genome replication by miR-199a(*).** *J Hepatol* 2009, **50(3)**:453-460.
13. Enomoto N, Sakuma I, Asahina Y, Kurosaki M, Murakami T, Yamamoto C, Ogura Y, Izumi N, Marumo F, Sato C: **Mutations in the nonstructural protein 5A gene and response to interferon in patients with chronic hepatitis C virus 1b infection.** *N Engl J Med* 1996, **334(2)**:77-81.
14. Akuta N, Suzuki F, Kawamura Y, Yatsuji H, Sezaki H, Suzuki Y, Hosaka T, Kobayashi M, Kobayashi M, Arase Y, Ikeda K, Miyakawa Y, Kumada H: **Prediction of response to pegylated interferon and ribavirin in hepatitis C by polymorphisms in the viral core protein and very early dynamics of viremia.** *Intervirology* 2007, **50(5)**:361-368.
15. Asselah T, Bieche I, Narguet S, Sabbagh A, Laurendeau I, Ripault MP, Boyer N, Martinot-Peignoux M, Valla D, Vidaud M, Marcellin P: **Liver gene expression signature to predict response to pegylated interferon plus ribavirin combination therapy in patients with chronic hepatitis C.** *Gut* 2008, **57(4)**:516-524.
16. Feld JJ, Nanda S, Huang Y, Chen W, Cam M, Pusek SN, Schweigler LM, Theodore D, Zacks SL, Liang TJ, Fried MW: **Hepatic gene expression during treatment with peginterferon and ribavirin: Identifying molecular pathways for treatment response.** *Hepatology* 2007, **46(5)**:1548-1563.
17. Chen L, Borozan I, Feld J, Sun J, Tannis LL, Coltescu C, Heathcote J, Edwards AM, McGilvray ID: **Hepatic gene expression discriminates responders and nonresponders in treatment of chronic hepatitis C viral infection.** *Gastroenterology* 2005, **128(5)**:1437-1444.
18. Tanaka Y, Nishida N, Sugiyama M, Kurosaki M, Matsuura K, Sakamoto N, Nakagawa M, Korenaga M, Hino K, Hige S, Ito Y, Mita E, Tanaka E, Mochida S, Murawaki Y, Honda M, Sakai A, Hiasa Y, Nishiguchi S, Koike A, Sakaida I, Imamura M, Ito K, Yano K, Masaki N, Sugauchi F, Izumi N, Tokunaga K, Mizokami M: **Genome-wide association of IL28B with response to pegylated interferon-alpha and ribavirin therapy for chronic hepatitis C.** *Nature genetics* 2009, **41(10)**:1105-1109.
19. Younossi ZM, Baranova A, Afendy A, Collantes R, Stepanova M, Manyam G, Bakshi A, Sigua CL, Chan JP, Iverson AA, Santini CD, Chang SY: **Early gene expression profiles of patients with chronic hepatitis C treated with pegylated interferon-alfa and ribavirin.** *Hepatology* 2009, **49(3)**:763-774.
20. Dudoit S, Fridlyand J: **A prediction-based resampling method for estimating the number of clusters in a dataset.** *Genome Biol* 2002, **3(7)**: RESEARCH0036.
21. Dudoit S, Fridlyand J: **Bagging to improve the accuracy of a clustering procedure.** *Bioinformatics* 2003, **19(9)**:1090-1099.
22. **National Institutes of Health Consensus Development Conference Statement: Management of hepatitis C: 2002–June 10-12, 2002.** *Hepatology* 2002, **36(5 Suppl 1)**:S3-20.
23. Ferenci P, Fried MW, Shiffman ML, Smith CI, Marinos G, Goncales FL, Haussinger D, Diago M, Carosi G, Dhumeaux D, Craxi A, Chaneac M, Reddy KR: **Predicting sustained virological responses in chronic hepatitis C patients treated with peginterferon alfa-2a (40 KD)/ribavirin.** *J Hepatol* 2005, **43(3)**:425-433.
24. Sonkoly E, Stahle M, Pivarcsi A: **MicroRNAs and immunity: novel players in the regulation of normal immune function and inflammation.** *Seminars in cancer biology* 2008, **18(2)**:131-140.
25. Lindsay MA: **microRNAs and the immune response.** *Trends in immunology* 2008, **29(7)**:343-351.
26. Chen PY, Manninga H, Slanchev K, Chien M, Russo JJ, Ju J, Sheridan R, John B, Marks DS, Gaidatzis D, Sander C, Zavolan M, Tuschl T: **The developmental miRNA profiles of zebrafish as determined by small RNA cloning.** *Genes & development* 2005, **19(11)**:1288-1293.
27. Peng X, Li Y, Walters KA, Rosenzweig ER, Lederer SL, Aicher LD, Proll S, Katze MG: **Computational identification of hepatitis C virus associated microRNA-mRNA regulatory modules in human livers.** *BMC Genomics* 2009, **10**:373.
28. Gong AY, Zhou R, Hu G, Li X, Splinter PL, O'Hara SP, LaRusso NF, Soukup GA, Dong H, Chen XM: **MicroRNA-513 regulates B7-H1 translation and is involved in IFN-gamma-induced B7-H1 expression in cholangiocytes.** *J Immunol* 2009, **182(3)**:1325-1333.
29. Yu D, Rao S, Tsai LM, Lee SK, He Y, Sutcliffe EL, Srivastava M, Linterman M, Zheng L, Simpson N, Ellyard JI, Parish IA, Ma CS, Li QJ, Parish CR, Mackay CR, Vinuesa CG: **The transcriptional repressor Bcl-6 directs T follicular helper cell lineage commitment.** *Immunity* 2009, **31(3)**:457-468.
30. Hsu PW, Lin LZ, Hsu SD, Hsu JB, Huang HD: **ViTa: prediction of host microRNAs targets on viruses.** *Nucleic acids research* 2007, **35(Database issue)**:D381-385.
31. Pulendran B, Tang H, Denning TL: **Division of labor, plasticity, and crosstalk between dendritic cell subsets.** *Curr Opin Immunol* 2008, **20(1)**:61-67.
32. Wertheimer AM, Bakke A, Rosen HR: **Direct enumeration and functional assessment of circulating dendritic cells in patients with liver disease.** *Hepatology* 2004, **40(2)**:335-345.
33. Dienstag JL, McHutchison JG: **American Gastroenterological Association technical review on the management of hepatitis C.** *Gastroenterology* 2006, **130(1)**:231-264.

Pre-publication history
The pre-publication history for this paper can be accessed here:
http://www.biomedcentral.com/1755-8794/3/48/prepub

doi:10.1186/1755-8794-3-48
Cite this article as: Murakami *et al.*: **Hepatic microRNA expression is associated with the response to interferon treatment of chronic hepatitis C.** *BMC Medical Genomics* 2010 **3**:48.

Polyubiquitin conjugation to NEMO by triparite motif protein 23 (TRIM23) is critical in antiviral defense

Kei-ichiro Arimoto[a,b], Kenji Funami[c], Yasushi Saeki[d], Keiji Tanaka[d], Katsuya Okawa[e], Osamu Takeuchi[f], Shizuo Akira[f], Yoshiki Murakami[b], and Kunitada Shimotohno[c,1]

[a]Laboratory of Biological Protection, Institute for Virus Research, Graduate School of Medicine, Kyoto University, Shogo-in, Sakyo-ku, Kyoto 606-8507, Japan; [c]Research Institute, Chiba Institute of Technology, 2-17-1, Tsudanuma, Narashino City, Chiba 275-0016, Japan; [d]Laboratory of Frontier Science, Core Technology and Research Center, Tokyo Metropolitan Institute of Medical Science, 2-1-6, Kamikitazawa, Setagaya-ku, Tokyo 156-8506, Japan; [e]Kyowa Hakko Kirin Co., Ltd., Takasaki City, Sunto-gun, Shizuoka 411-8731, Japan; [f]Laboratory of Host Defense, World Premier International Immunology Frontier Research Center, Research Institute for Microbial Diseases, Osaka University, 3-1 Yamada-oka, Suita, Osaka 565-0871, Japan; and [b]Center for Genomic Medicine, Kyoto University, Shogo-in, Sakyo-ku, Kyoto 606-8507, Japan

Edited by Diane E. Griffin, Johns Hopkins Bloomberg School of Public Health, Baltimore, MD, and approved July 16, 2010 (received for review April 8, 2010)

The rapid induction of type I IFN is a central event of the innate defense against viral infections and is tightly regulated by a number of cellular molecules. Viral components induce strong type I IFN responses through the activation of toll-like receptors (TLRs) and intracellular cytoplasmic receptors such as an RNA helicase RIG-I and/or MDA5. According to recent studies, the NF-κB essential modulator (NEMO, also called IKKγ) is crucial for this virus-induced antiviral response. However, the precise roles of signal activation by NEMO adaptor have not been elucidated. Here, we show that virus-induced IRF3 and NF-κB activation depends on the K(lys)-27-linked polyubiquitination to NEMO by the novel ubiquitin E3 ligase triparite motif protein 23 (TRIM23). Virus-induced IRF3 and NF-κB activation, as well as K27-linked NEMO polyubiquitination, were abrogated in TRIM23 knockdown cells, whereas TRIM23 knockdown had no effect on TNFα-mediated NF-κB activation. Furthermore, in NEMO-deficient mouse embryo fibroblast cells, IFN-stimulated response element-driven reporter activity was restored by ectopic expression of WT NEMO, as expected, but only partial recovery by NEMO K165/309/325/326/344R multipoints mutant on which TRIM23-mediated ubiquitin conjugation was substantially reduced. Thus, we conclude that TRIM23-mediated ubiquitin conjugation to NEMO is essential for TLR3- and RIG-I/MDA5-mediated antiviral innate and inflammatory responses.

innate immunity | signal transduction | virus infection

Upon viral infection, host cells recognize the viral components and activate innate immune signaling to exert antiviral responses (1–4). RIG-I and/or MDA5 sense viral dsRNA (5–8) and are recruited to another antiviral signaling adaptor, IPS-1 (also called MAVS, Cardif, or VISA) (9–12). IPS-1 directly interacts with TRAF3 and triggers auto-ubiquitination of TRAF3, which then activates TBK1 and IKKε, leading to activation of transcription factors NF-κB and IRF3 (13, 14). A recent study indicated that NEMO acts upstream of TBK1 and IKKε and is essential for virus-induced TLR3- and RIG-I/MDA5–mediated antiviral activation (15).

Because rapid induction of type I IFN expression is the key process in initiating the innate antiviral response, clarification of NEMO-mediated antiviral signaling is important for understanding innate immune signaling; however, NEMO-mediated antiviral signaling is not well elucidated. Recent studies indicate that several ubiquitin E3 ligases are involved in the regulation of innate immune signaling (16–21). We identified the ubiquitin E3 ligase TRIM23 (Triparite motif protein 23), also named ADP ribosylation factor domain protein 1 (ARD1), which was reported to have E3 ligase activity in vitro (22), that functioned as an E3 ligase for NEMO ubiquitin conjugation. TRIM23 exerts a potent antiviral state following its overexpression. Furthermore, we demonstrated that antiviral activity depends not on K(Lys)63-linked but on K27-linked polyubiquitin conjugation to multiple sites of NEMO by TRIM23 expression. Virus-induced IRF3 and NF-κB activation, as well as K27-linked NEMO polyubiquitination, were abrogated in TRIM23 knockdown cells (including primary mouse embryonic fibroblasts), whereas TRIM23 knockdown had no effect on TNFα-mediated NF-κB activation.

Results

TRIM23 Interacts with NEMO. Recent studies indicate that several ubiquitin E3 ligases are involved in the regulation of innate immune signaling (16–21). We previously reported that the E3 ubiquitin ligase RNF125 negatively regulates RIG-I signaling (17), and it has been reported that RNF125 is also a T-cell activator (23), which suggests the presence of plural functions of RNF125 in regulation of cell proliferation. To identify genes affected by RNF125, we conducted microarray analysis (mock- vs. RNF125-transfected 293T cells) and found the gene for TRIM23 up-regulated ~3-fold (Fig. S1*A*). Through analysis of function of TRIM23, we also found that TRIM23 up-regulated the NF-κB–driven reporter gene in cells expressing NEMO. Introduction of TRIM23 slightly activated NF-κB in cells expressing endogenous NEMO and substantially activated NF-κB in cells ectopically expressing NEMO. Furthermore, we found that NEMO migrated slowly by SDS/PAGE when coexpressed with TRIM23 (Fig. S1*B*), suggesting posttranslational modification, most likely ubiquitin conjugation by TRIM23. It has been reported that TRIM23 has E3 ligase activity in vitro (22). Because ubiquitin E3 ligases generally require association with the substrate to execute its enzyme activity, we analyzed the association of TRIM23 with NEMO by GST-pulldown and coimmunoprecipitation assays. These results showed that TRIM23 interacted with NEMO directly (Fig. S1*C*). Deletion analysis of NEMO showed that both the CC1 and LZ domains of NEMO are essential for this interaction (Fig. 1 *A* and *C*). Binding analysis showed further that the TRIM23 C-terminal ARF domain interacted with NEMO CC1 and LZ domains as effectively as the full-length TRIM23, whereas the RING finger and B-box/B-box/CCD domains did not (Fig. 1 *A*, *B*, and *D*). Bifluorescent complementation analysis also revealed interaction of NEMO with TRIM23 in living HeLa cells (Fig. 1*E*). An interaction between endogenous NEMO and TRIM23 was also detected in 293T cells (Fig. 1*F*).

TRIM23 Is an E3 Ligase for Conjugation of K27 Type Ubiquitin to NEMO. To examine whether TRIM23 ubiquitinates NEMO, NEMO-FLAG was coexpressed with WT TRIM23 or its E3 ligase activity-defective RING mutants (TRIM23C34A and TRIM23ΔRING). Although TRIM23 expression markedly increased the ubiquitin conjugation levels of NEMO-FLAG, neither TRIM23C34A nor TRIM23ΔRING had any effect (Fig. 2*A*). Levels of ubiquitin conjugation to NEMO were enhanced by increasing amounts of TRIM23. Under these conditions, the mRNA levels of NEMO, GAPDH, and tubulin were unchanged (Fig. 2*B*). By analyzing mutants of ubiquitin for conjugation to NEMO in a TRIM23-dependent manner, we observed that the K27-only type could be

Author contributions: K.-i.A., K.F., and K.S. designed research; K.-i.A. performed research; O.T., S.A., and Y.M. contributed new reagents/analytic tools; K.-i.A., K.F., Y.S., K.T., K.O., O.T., S.A., Y.M., and K.S. analyzed data; and K.-i.A. and K.S. wrote the paper.

The authors declare no conflict of interest.

This article is a PNAS Direct Submission.

[1]To whom correspondence should be addressed. E-mail: kunitada.shimotono@it-chiba.ac.jp.

This article contains supporting information online at www.pnas.org/lookup/suppl/doi:10.1073/pnas.1004621107/-/DCSupplemental.

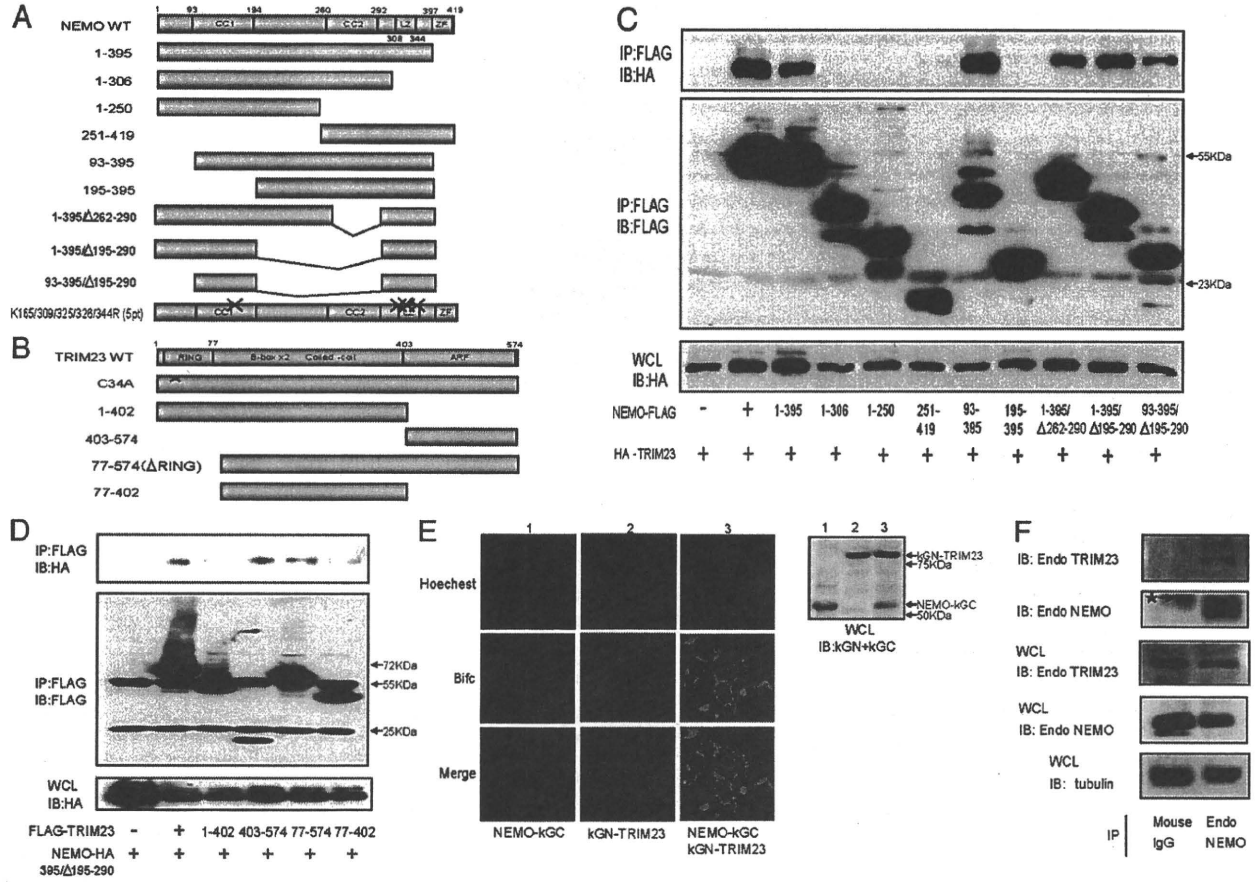

Fig. 1. Interaction between NEMO and TRIM23. (*A* and *B*) Schematic drawings of NEMO, TRIM23, and their derivatives used in this work. CC1 coiled-coil domain 1; CC2, coiled-coil domain 2; LZ, leucine zipper; ZF, zinc finger. RING finger domain, B-box-B-box/CCD (coiled-coil domain), and ARF (ADP ribosylation factor) domain in TRIM23 are shown. X indicates sites of mutagenesis described in the text. (*C*) 293T cells were cotransfected with plasmids encoding HA-TRIM23 and NEMO-FLAG or its mutants. (*D*) NEMO CC1 and LZ domains interacted with the TRIM23 ARF region in 293T cells. (*E*) HeLa cells were transfected with plasmids encoding NEMO-kGC and kGN-Mock, kGN-TRIM23 and Mock-kGC, or NEMO-kGC and kGN-TRIM23. Nuclear localizations were detected by Hoechst 33342. Bifc signal revealed TRIM23-NEMO–specific association. Expression of NEMO and TRIM23 in HeLa cells were also confirmed by immunoblot using anti-kGN and -KGC antibody. (*F*) Interaction of endogenous NEMO with endogenous TRIM23 in 293T cells 24 h after SV infection. Asterisk denotes nonspecific band.

conjugated as polyubiquitin to NEMO (Fig. 2*C*). This was further confirmed by the ubiquitin conjugation of K63R, but not of K27R mutant of ubiquitin (Fig. 2*D*). NF-κB reporter activity in cells ectopically expressing K27-only ubiquitin was higher when compared with K27R ubiquitin in NEMO and TRIM23 expressing 293T cells (Fig. 2*E*). An in vitro ubiquitination assay showed that TRIM23 could use UbcH1, 5a, 5b, 5c, and 13/Mms2 as an ubiquitin E2-conjugating enzyme (Fig. S2*A*). Among these E2 enzymes, the presence of UbcH5s could conjugate ubiquitin to NEMO at shorter time of reaction, suggesting that the presence of UbcH5s, rather than UbcH1 or Ubc13/Mms2, may have a strong ability to conjugate ubiquitin to NEMO. When using the K27-only ubiquitin mutant, only UbcH5a, 5b, and 5c showed ubiquitin conjugation activity, suggesting that these may be the major E2 enzymes functioning in vivo (Fig. S2*B*).

In the analysis using deletion mutants of NEMO, it was observed that TRIM23 could conjugate ubiquitin preferentially to the NEMO CC1 and LZ domains (Fig. S3*A*). Single point mutation of K to R in these domains of WT-NEMO was not affected by TRIM23 expression at the ubiquitin conjugation level (Fig. S3*B*). In an analysis of several NEMO mutants having mutations on plural lysine residues in these domains of NEMO, we observed that ubiquitin conjugation to NEMO K165/309/325/326/344R, NEMO-5pt, was substantially reduced when compared with that of the WT NEMO. This suggests the importance of these five lysine residues in TRIM23-dependent ubiquitin conjugation to NEMO, at least in part (Fig. 2*F*).

TRIM23 Exerts a Potent Antiviral State Following Its Overexpression. NEMO has critical roles in virus-induced innate and inflammatory responses (15). To investigate the roles of TRIM23-mediated NEMO ubiquitination, we examined IFNβ, ISRE, or NF-κB promoter-driven reporter activity by expressing TRIM23 or TRIM23C34A after treating cells with poly I:C, infection with Sendai virus (SV), or coexpressing upstream adaptor molecules of innate immunity signaling. Ectopic expression of WT TRIM23, together with plasmids encoding TLR3, RIG-I, or IPS1, upregulated ISRE reporter activity. Expression of TRIM23C34A suppressed the reporter activity (Fig. S4A). Same results were observed in both IFNβ and NF-κB reporter assays with polyI:C or SV infection (Fig. S4 *B* and *C*). Consistent with the NEMO ubiquitination level (Fig. 2*B*), NF-κB promoter activity considerably increased and decreased dose-dependently with TRIM23 and TRIM23C34A expression, respectively (Fig. S4*D*). Reduction of the reporter activity by TRIM23C34A seems to have a dominant negative effect on endogenous TRIM23, although the precise mechanism requires further clarification.

Suppression of TRIM23 Impaired K27-Linked Ubiquitin Conjugation to NEMO and Virus-Induced Antiviral Activity. To examine the physiological roles of TRIM23 in antiviral innate immunity, we analyzed IFNβ and NF-κB reporter activity in cells knocked-down of TRIM23 by specific siRNA. We also established 293T cells that were knocked down TRIM23 constitutively (Fig. 3*A*). TRIM23 knockdown impaired IFNβ reporter activity by SV infection and